A STUDY OF THE ELECTRONIC TRANSITIONS OF A PORPHYRIN DIMER

By

HUNG THE DOAN

Bachelor of Science, 2013

Texas Christian University

Fort Worth, Texas

Master of Science, 2016

Texas Christian University

Fort Worth, Texas

Submitted to the Graduate Faculty of the

College of Science and Engineering

Texas Christian University

in partial fulfillment of the requirements

for the degree of

Doctoral of Philosophy

August 2018

ACKNOWLEDGMENTS

This research would not have been possible without the support of the Texas Christian University College of Science and Engineering, and the Department of Physics and Astronomy. I want to first thank the Chairman of my committee, Dr. Zygmunt Gryczynski. As my teacher and research advisor, he has taught me more than I could ever express with words and showed me what a good scientist and a good person should be. I also want to thank each member of my committee, Dr. Peter Frinchaboy, Dr. Hana Dobrovolny, and Dr. Anton Naumov who have supported ing my research and provided me suggestions and discussions to pursue my goals. I would like to thank Dr. Sergei Dzyuba and Dr. Milan Balaz, our collaborators, who synthetize the molecule and provide great guidance and helpful criticsism throughout this project.

Five years was not too long but definitely not a short time. It was a great journey, and I was never alone. My biggest thanks to the most important people in my pursuit of this project, my parents. Thank you, mom and dad, for your love and guidance that are with me in what I do. Thank you for always be there for me physically and emotionally. Thank you for always supporting my decisions no matter how difficult they are. This Ph.D. is dedicated to you.

I am grateful to all of those with whom I have had the pleasure to work during this project. I would like to thank Dr. Joseph Kimball for his help and endless conversations regarding this research as my lab partners and good friends in the last five years. I also want to thank Dr. Sangram Raut and Dr. Sebastian Requena, and for their help and support. I wish to thank my graduate fellow students for their support and advising throughout the years. Lastly, I would like to thank all of my friends and family members for their never-ending support and belief.

TABLE OF CONTENTS

LIST OF FIGURES

LIST OF TABLES

LIST OF ABBREVIATIONS

PD – Porphyrin dimer

FCS - Fluorescence correlation spectroscopy

FRAP - Fluorescence recovery after photobleaching

SPT - Single particle tracking

PDT - Photodynamic therapy

ROS - Reactive oxygen species

LD - Linear dichroism

UV - Ultra-violet

IR - Infrared

TCSPC - Time-correlated single photon counting

PMT - Photomultiplier tube

HOMO - Highest occupied molecular orbital

LUMO - Lowest unoccupied molecular orbital

MALDI-TOF - Matrix-assisted laser desorption/ionization time-of-flight

HPLC - High performance liquid chromatography

PVA - Polyvinyl alcohol

DMSO - Dimethyl sulfoxide

MCP - Microchannel plate

EM - Emission

Chapter 1 Introduction

Naturally occurring porphyrins have a wide variety of derivatives that are involved in many critical biological processes. Porphyrins exhibit useful spectroscopic properties and are frequently utilized as probes and photosensitizers in cancer therapy. A recently developed porphyrin derivative called "Porphyrin Dimer" (PD) is a new and interesting molecule that consists of two conjugated porphyrin units. This dimer presents favorable photophysical properties, namely an enormous extinction coefficient, good photostability, and shows high intracellular accumulation. Furthermore, these two porphyrin moieties have the unique ability to rotate around its diyne moiety, thus forming a so-called "molecular rotor." This physical process (rotation) from planar to non-planar conformation (and vice-versa) is associated with a significant change in its molecular orbitals and presents an easily detectable change in its fluorescence properties [1,2]. Importantly, the rings' rotation can be robustly hindered by their surroundings, and especially the solvent's microviscosity. This means the PD molecular rotor is highly capable of reporting on its local environment's viscosity.

Viscosity is an essential characteristic of a microenvironment, and the viscosity of a cellular microenvironment becomes an especially important factor for our understanding of many physiological processes and diseases. Viscosity is also a principal factor determining the micro- and macroscopic properties of systems/solutions and a principal factor that can control the rates of processes and reactions on the microscopic scale. The need to detect microscopic viscosity is widely recognized throughout biochemical and biological research, and many new applications are emerging in physiology, material science, and atmospheric sciences. Methods that allow the detection of viscosity on a microscopic scale are fluorescence correlation spectroscopy (FCS),

fluorescence recovery after photobleaching (FRAP), single particle tracking (SPT), steady-state and time-resolved fluorescence anisotropy. Emerging potential applications in oncology relate to the fact that tumors have a profoundly hypoxic environment with very different cytoplasmic and extracellular viscosities than healthy cells and thus such a viscosity probe can report on cancer therapy progress. PD has also been shown to be an efficient photosensitizer for Photodynamic Therapy (PDT)[3-7]. Photodynamic Therapy[8-10] has become one of the most effective cancer treatments available today. PDT uses compounds called photosensitizers that upon excitation by light, produce[11] cytotoxic agents that can destroy a tumor or modify the growth of cancer tissue[12]. Over the past thirty years, PDT has gained a reputation as the fourth modality for cancer treatment after surgery, chemotherapy, and radiotherapy. The key advantage of PDT is the localized activation of the drug by precise light illumination and reducing the off-site toxicity to the healthy tissue/cells.

Various porphyrins have been broadly used as PDT agents[11,13]. A significant advantage is that many porphyrins naturally occur in the body and thus have minimal physiological toxicity. Many porphyrin derivatives, such as heme, are the byproducts of Protoporphyrin IX synthesis and degradation of hemoglobin in the human body. Also, most porphyrins are well soluble in water and can be easily modified to enhance the efficiency for producing toxic free radicals in the body. The key toxic radical is singlet oxygen that is produced when a porphyrin molecule in its excited state interacts with molecular oxygen (O_2) dissolved in tissue/cells. Typically, the reaction happens from the triplet state of the porphyrin, and it transfers its energy directly to oxygen to form singlet oxygen — a highly Reactive Oxygen Species (ROS)[14]. For this to occur, the energy and quantum mechanical properties of the porphyrin in its excited state must suit the oxygen's activation energy. Surprisingly, the activation energies for oxygen molecules in their triplet ground state are in the

far-red and near IR regions (800 nm – 1100 nm), which happen to nicely match the region of porphyrins' excited triplet state. Another advantage of porphyrins is the possibility of utilizing these red laser excitations (~600 nm – 700 nm) which can penetrate tissue up to a few millimeters, as opposed to more "blue" lasers, which tissue scatters much more effectively, and thus have a much smaller penetration depth.

To fully utilize PD as a cellular viscometer (rotor) and potentially as a photosensitizer in PDT it is critically important to understand the characteristics and photophysical properties of both of the major PD conformations. The spectroscopic properties of PD that remain unknown are the relative strengths and orientations of the transition dipole moments associated with the planar and twisted conformations. One crucial unanswered and typically un-asked question for using PD as a molecular rotor is why a wide range of experimentalists have selected an excitation that lays in the 470 nm - 480 nm range that is off-peak to the maximum of its Soret band. Our goal is to test if this is the optimal range and what the rationale is for this. These properties are crucial for the interpretation of PD's absorption and emission spectra as well as their interactions with other molecules. For example, the spectroscopic properties that are responsible for interactions with molecular oxygen are of significant interest because they may help us understand the formation of oxygen radicals for PDT.

The goal of these studies is to establish a new and robust method to determine the orientation and relative strengths of the transition moments for the planar and twisted conformers of PD. Interestingly, various methods to study the orientation of transition moments for absorption (linear dichroism – "LD") and emission (fluorescence anisotropy) have been developed in the last century[15-19]. Moreover, hundreds of molecules have been intensively investigated for application in PDT and as micro-viscometers. However, there is yet to be a study that explores the orientation

of the transition moments for a molecular rotor and most importantly how spectroscopic properties change upon molecular rotation.

There are four main obstacles that needed to be solved:

1. Immobilize and orient PD molecules.
2. Force PD molecules predominantly toward one conformation (planar or twisted).
3. Determine the transition moments' orientations for the dominant PD conformer.
4. Identify the electronic transitions most suitable for PD molecule to be used as a molecular rotor and potentially as a PDT sensitizer.

This work is the first attempt to assign the transition moments' directions of a dimeric molecular system with twisted and planar conformations. All systems studied up to now were composed of single organic molecules. LD and fluorescence anisotropy measurements are the key measurement techniques which enable us to assign PD electronic transitions. These properties are likely to play a fundamental role in optimizing molecular systems to be used as molecular rotors or as photo synthesizers for PDT, and the development of the next generation of rotors and photosensitizers.

Chapter 2 Basics of Light Interaction with Molecules

2.1 Perrin-Jablonski Diagram

We call "light" a small range of the broad spectrum of electromagnetic radiation that corresponds to the ultra-violet (UV), visible, and near infrared (IR) spectral range (200 nm – 1100 nm). The interaction between electromagnetic radiation ("light") and matter constitutes the basis for optical spectroscopy. The principal manifestation of this interaction is light absorption by molecules followed by the emission of a photon by the molecule. This process is called fluorescence. Measuring absorption of light by a molecule and the consequential light emitted by the molecule are the focus of this dissertation. The absorption and emission processes are typically described using the classic energetic representation of molecular energy levels called a Perrin-Jablonski diagram (historically called a Jablonski diagram), as shown in Figure 1.

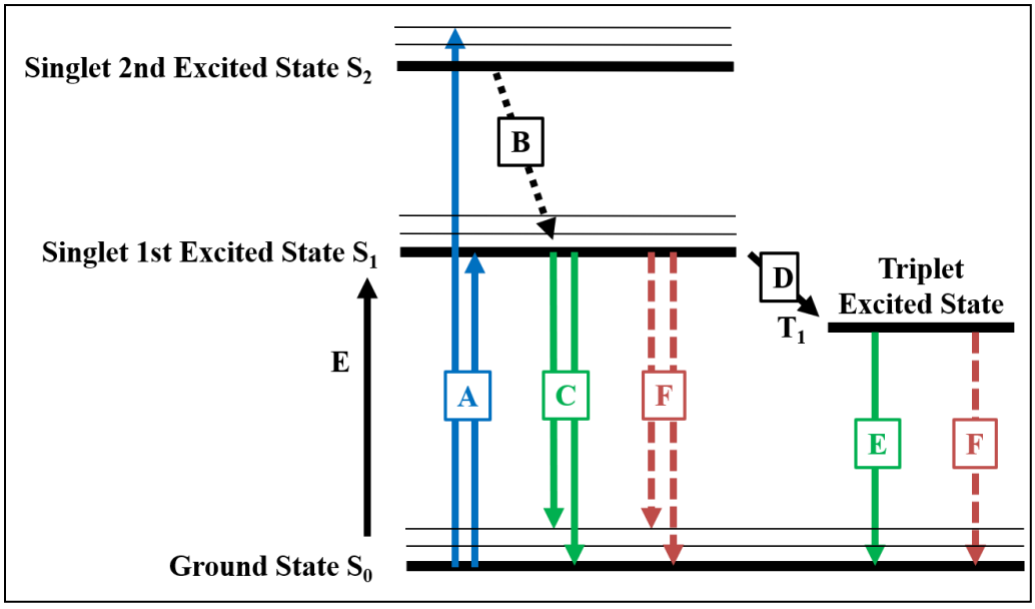

Figure 1: The Perrin-Jablonski diagram.

Atoms in organic molecules form molecular bonds where they share loosely bound electrons in their outer orbital shells. These shared electron clouds are responsible for the molecule's

interaction with light. The energy of molecular orbitals in a molecule is quantized similar to an atom's energy. In the initial state, without having any extra energy, the electrons are relaxed, and this is called the ground state, depicted in Figure 1 as S_0. Upon interacting with light, the molecule absorbs energy from light (photon) and converts this absorbed energy into the energy of the outer electrons. This is a speedy transition (process "A" in Figure 1) to one of the higher allowed molecular electronic energy states such as S_1 or S_2. These are the thick, black horizontal lines in Figure 1. Each of those electronic states (S_0, S_1…) contain many vibrational energy levels as well. Each level is associated with a quantized amount of energy due to the different vibration modes of the molecule, and are denoted as 0, 1, 2 and so on as seen as thin horizontal lines in Figure 1. The transition from the ground state to a higher electronic energy level is represented by the vertical blue arrows. This is what we call the process of light absorption. The absorption of a photon by a molecule is a rapid transition, on the order of ~10^{-15} s. With notably rare exceptions, the excited molecule quickly relaxes to the lowest vibrational level of the first excited state, S_1. This process is called internal relaxation and is depicted as "B" in Figure 1. The S_1 state is an allowed state and molecule may stay in this state for a finite duration of time before returning to one of the vibrational levels of the ground state, which then again quickly reaches thermal equilibrium in its lowest vibrational state. The transition from S_1 to S_0 can involve emission of a photon (process "C" in Figure 1) at a rate called the radiative decay rate, denoted as K_r or Γ, or without the emission of a photon at another rate called the non-radiative decay rate denoted as K_{nr} (labeled as "D" in Figure 1). For the sake of simplicity, molecules that can emit light are called fluorophores. The emitted light typically has a longer wavelength (lower energy) compared to that of the excitation (absorbed) light. The inherent wavelength difference between the absorbed light and emitted light is called the Stokes shift.

Very rarely, an excited molecule in the S_1 state can go through a spin conversion process to a triplet state, denoted as T_1 in Figure 1. The transition of S_1 to T_1, or process "F", is called "intersystem crossing." The transitions from T_1 to the ground state (E) are forbidden. Therefore, the rate constant for emission from T_1 is several orders of magnitude smaller than that for fluorescence. This phenomenon is termed phosphorescence[20].

Fluorescence detection is considered one of the most sensitive technologies that are widely available today, with the capability of detecting a single molecule. This incredible sensitivity, achievable with harmless radiation (visible and near-IR light), has generated many applications in biology, ranging from cellular and tissue imaging, to even environmental studies. Importantly, red and NIR light can deeply penetrate tissue and is very attractive for PDT applications. On the other hand, porphyrins (including PD) are good absorbers in the red spectral range that serve as an attractive advantage for photosensitizers. To improve PDT applications, we need to understand the underlying mechanisms responsible for the formation of ROS to rationally enhance their efficiency.

2.2 Light Polarization

The polarization of light is the direction of its electric field oscillation. Most light in everyday life has no constraints regarding the plane of the light's polarization. For example, the direction of the electric field of any given light wave from the Sun has an arbitrary direction in the plane orthogonal to the direction of light propagation. Thus, any two or more photons emanating from the Sun very likely have different electric field directions, and thus the light coming from the Sun has randomly distributed electric field vectors around the direction of its propagation. This we call an isotropic light. A single wave (single photon) has only one orientation of its electric field (one plane), and any talk of linear polarization is trivial.

When light passes through a polarizer (Figure 2a, blue circle), a device which only allows light of a particular polarization to be transmitted (say $\hat{r}$, represented by the parallel lines inside the polarizer), it may lose some or all of its intensity. If an electric field vector, $\vec{E}$ points along $\hat{r}$ with no intensity is lost, the light is already polarized. If E and $\hat{r}$ are orthogonal, then all of the intensity is lost (no light travels passed the polarizer). If $\vec{E}$ and $\hat{r}$ are neither parallel nor orthogonal, then the amount of light transmitted is determined by Malus' Law,

$$I = I_0 cos^2\left(\frac{\vec{E}\cdot\hat{r}}{|\vec{E}||\hat{r}|}\right) = I_0 cos^2(\hat{r}\cdot\ \hat{e}) = I_0 cos^2(\alpha), \tag{1}$$

where α is the angle between the polarizer polarization direction and E of the incident light. Upon passing through a polarizer, the polarizations of isotropic light can be averaged and treated as two orthogonal components, one parallel and the other perpendicular to the polarization axis of the polarizer. Therefore, isotropic light loses half of its intensity traveling through a polarizer. It is important to remember that light has no memory of its previous states including information about polarization. A typical example of this is light passing through two orthogonal polarizers ($\theta = 90^o$) where there is no light transmitted (Figure 2b). However, when there is a third polarizer inserted in-between the two orthogonal polarizers light is indeed transmitted (Figure 2c).

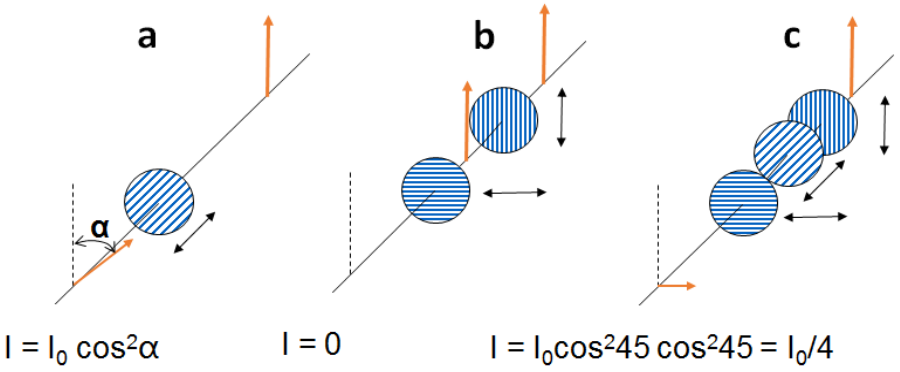

Figure 2 Light transmission through polarizers. Light is traveling out of the page and downward.

To illustrate this mathematically consider light which passed through the first polarizer and now enters the orthogonal one.

$$I_{final} = I_0 cos^2(90) = 0. \quad (2)$$

As expected no light is transmitted. However, in the presence of a third intermediate polarizer which is offset 45 degrees to both original polarizers the final intensity becomes

$$I_{intermediate} = I_0 cos^2(45) = {}^1\!/_2\, I_0, \quad (3)$$

$$I_{final} = {}^1\!/_2\, I_0 cos^2(45) = {}^1\!/_4\, I_0. \quad (4)$$

Light is indeed transmitted for any angle in-between 0^o and 90^o. Thus, light entered both systems in the same state and left through the same final polarizer, but its final intensity varied significantly due to the presence of a third polarizer in one of the systems. The reason for this is that after the light passed through the intermediate polarizer in the second example all information about its original state was completely forgotten. Usually polarized light is a collection (ensemble) of light waves (may be called photons) which all have the same direction of the electric field.

2.3 Absorption

The primary factors responsible for light absorption by molecules are:

1. The energy of the incident photon must correspond to the energy difference of two given states, which we can represent as $h\nu = S_i - S_0$
2. The strength of the absorption oscillator, called the transition moments. This is manifested by the absorption cross-section, σ, of a given molecule (fluorophore). This parameter reflects the probability of a photon passing in the molecule's proximity to be absorbed. In chemistry, it is referred to as the extinction coefficient, ε.
3. The concentration of the molecules.

4. The intensity of the excitation light source, which dictates the number of molecules being excited.
5. The relative orientation between the polarization of the excitation light and the molecular transition moment. Transition moments have well-defined directions in a molecular framework, and thus, the probability for interacting with the incoming light depends on $cos^2\,\alpha$, where α is the angle between the transition moment direction and the plane of light polarization.

The concentration of molecules in a solution, *C*, is typically given in moles per liter [mol/L]. The number of molecules per cubic centimeter [number of molecules/cm^3] can be calculated using Avogadro's number (N_A - 6.0225×10^{23} mol^{-1}) and the conversion factor from [mol/L] as $C*N_A$ /1000. The absorption cross section of a molecule at a given wavelength λ is σ(λ), and it has units of [cm^2/mol]. The absorption cross-section reflects the probability for a photon of a given wavelength (energy) to be absorbed as it passes the fluorophore's proximity. We need to remember that a typical molecule is much smaller than the wavelength of light and the incoming/passing electromagnetic radiation produces a local field perturbation. A fluorophore in such a field has a certain probability of absorbing the energy which depends on the wavelength, or frequency of the field. As light travels through the solution and encounters a suspension of fluorophores, it will get absorbed by the individual fluorophore, and the number of absorbed photons will depend on the number of fluorophores in the light's path. In typical conditions, one fluorophore absorbs one photon, and the number of absorbed photons will be proportional to the length light travels through the solution, Δl. Thus, the change in intensity, ΔI, of the light as it travels through the solution is:

$$\Delta I = I_0 n \Delta l \sigma, \tag{5}$$

where I_0 is the intensity of the incoming light wave (number of photons per surface unit per second), and Δl is the path length, n is the number of fluorophores per unit of volume. The intensity of the transmitted light, I for a sample of thickness l is

$$I = I_0 e^{-\sigma n l}. \tag{6}$$

Equation (6) is known as the Beer-Lambert law. It is useful to rewrite the Beer-Lambert law as a function of wavelength because the absorption cross section is wavelength dependent

$$I(\lambda) = I_0(\lambda) e^{-\sigma(\lambda) n l}. \tag{7}$$

Absorption may be calculated using log base 10 or log base e, called decadic or Napierian, respectively. In photochemistry and photobiology, the extinction coefficient $\varepsilon(\lambda)$ is more frequently used. The extinction coefficient is a measure of how much a fluorophore at a concentration of 1 mole in a 1 cm layer absorbs at a particular wavelength. The units for the molar extinction coefficient are [L mol^{-1} cm^{-1}], although the units used may vary by field (i.e., [m^2 mol^{-1}]). In this text, the decadic molar extinction coefficient, $\varepsilon(\lambda)$, is used. It relates to the absorption cross section as

$$\sigma(\lambda) = \frac{2.303\ \varepsilon(\lambda)}{N_A} = 3.823 * 10^{-21}\ \varepsilon(\lambda) \tag{8}$$

Thus, as a general rule, when the absorption cross-section σ is used, then the natural logarithm will also be used. When the extinction coefficient ε is used, the logarithm will be taken with base 10. The Beer-Lambert law then becomes

$$I(\lambda) = I_0(\lambda) 10^{-\varepsilon(\lambda) C l}, \tag{9}$$

where C is the molar concentration of the molecule and the exponent's base is ten instead of e. One must be aware of this, as this convention is not adopted by all texts. The absorbance "Abs" or sometimes referred to as the optical density (OD), is defined as

$$Abs(\lambda) = \varepsilon(\lambda)Cl. \quad (10)$$

Absorbance is a unit-less quantity, which is the argument of the exponent in the Beer-Lambert law.

2.4 Transition Dipole Moment and Linear Dichroism (LD)

2.4.1 Transition Dipole Moment

A transition between energy levels requires a quantized amount of energy. However, not every transition is possible if it violates the Pauli Exclusion Principle, which states that an allowed transition cannot produce a configuration with three electrons existing in the same orbital. Furthermore, there are additional restrictions for a transition to take place. Those restrictions come from the nature of the interaction between electromagnetic radiation and matter, which are summarized by the selection rules. Light is considered an electromagnetic wave is having an electromagnetic field consisting of orthogonally oscillating electric and magnetic fields. The electric field interacts with the electric charges and is the primary factor responsible for electronic transitions. We can obtain the energy of an interaction between the electric field and a system of charged particles by calculating the scalar product of the electric field vector $\hat{\varepsilon}$ and the dipole moment vector $\hat{\mu}$ of the system.

$$\mathrm{E} = -\hat{\mu} \cdot \hat{\varepsilon}. \quad (11)$$

The dipole moment vector μ is defined as the summation of the product of each charged particle q_i and its corresponding position vector r_i,

$$\hat{\mu} = \sum_i q_i \cdot \hat{r}_i. \tag{12}$$

The expectation value for the interaction energy *E* can be calculated as

$$< E >= \int \psi_n^* (-\hat{\mu} \cdot \hat{\varepsilon}) \psi_n d\tau, \tag{13}$$

where $\int d\tau$ refers to integration over all coordinates. $\psi_n and\ \psi_n^*$ are the normalized state vector and its Hermitian conjugate state vector, respectively. Operators $\hat{\mu}$ and $\hat{\varepsilon}$ are vectors with the magnitude of the classical quantities μ and ε.

For visible light that has a wavelength much longer than the length of a molecule, the magnitude of the electric field can be seen as a constant over the length of the molecule. Therefore, the component ε can be taken out of the integral, leaving the expectation value for the permanent dipole moment of the molecules in state *n* as

$$< \mu >= \int \psi_n^* (-\hat{\mu}) \psi_n d\tau. \tag{14}$$

Thus, the energy of the interaction depends on the dipole moment of the system's charge distribution.

We are particularly interested in the transition between states and the corresponding strength of the interaction's energy. Therefore, we use the transition dipole moment as a substitute for the dipole moment. The transition dipole moment integral is very similar to the integral of the dipole moment. The difference lies in the two distinguished wave-functions, which are the initial (ψ_i) and final (ψ_f) states,

$$< \mu_T >= \int \psi_f^* (-\hat{\mu}) \psi_i d\tau = \mu_T. \tag{15}$$

In the case of $\mu_T = 0$, the transition is said to be forbidden, or electric dipole forbidden. If $\mu_T > 0$, the transition is allowed[21].

2.4.2 Linear Dichroism and the Dichroic Ratio

A molecule typically has multiple dipole transition moments which correspond to transitions of different electronic states of the molecule. Upon interacting with light, a molecule will preferentially absorb light with a plane of polarization of the electric field parallel to the direction of its transition moment. For an ensemble of oriented or partially oriented molecules, this means the absorption of light will depend strongly on the light polarization. If the direction of the fluorophore's orientation is defined as Z, the difference in absorption between light polarized parallel to Z and light polarized perpendicular to Z is called linear dichroism (LD),

$$LD = Abs_{\parallel} - Abs_{\parallel}, \tag{16}$$

where $Abs_{\parallel}$ and $Abs_{\parallel}$ represent parallel and perpendicular to absorption component directions. It is difficult to measure the absorption properties of a single molecule. Therefore, we frequently utilize a macroscopically oriented system. There are many oriented or partially oriented systems - such as crystals, liquid crystals, oriented membranes, and stretched polymer films. Such systems enforce the embedded molecules' orientation. This research utilizes a very convenient approach to align fluorophores by embedding them into a polymer then stretching the polymer. Poly(vinyl) alcohol (PVA) is a transparent polymer that can be easily stretched multiple-fold in length, thus inducing a significant orientation of elongated and planar molecules. The process of stretching PVA film aligns the polymer chains along the stretching direction. Subsequently, the realigned polymer chains force the fluorophores to align their long molecular axis along with the stretching direction. The fluorophores orientation directly depends on the stretching ratio $R_s = \frac{a}{b}$, where a is

the semi-major axis, and b is the minor axis of an ellipsoid deformed from an initial sphere envisioned in isotropic film[22-24].

Once we have the oriented films, we measure their two absorption components for light polarization parallel ($\parallel$) to the stretching direction, $Abs_{\parallel}$, and perpendicular ($\perp$) to it, $Abs_{\perp}$. Linear dichroism is calculated using Eq. (16). The dichroism of light absorption can also be presented in the form of a dichroic ratio R_d,

$$R_d = \frac{Abs_{\parallel}}{Abs_{\perp}}. \tag{17}$$

In general, the value obtained from the dichroic ratio provides valuable information about the conformation and orientation structure of the molecules in an oriented system such as a stretched PVA film. More specifically, when using the appropriate model, the dichroic ratio can distinguish different transition dipole moments within the molecular structure, as well as their relative orientation to each other. For an elongated molecule (rod-like) with a known molecular axis, the dichroic ratio can identify the orientation of the transition dipole moment that is either co-linear or offset by a certain degree off of the molecular axis. For a planar system with multiple transition dipole moments, the dichroic ratio can classify the in-plane and out-of-plane transitions.

Chapter 3 Fluorescence

3.1 The Emission

Similar to atoms, the character of a molecular system depends on the spin of its electrons. Molecular systems consist of molecular orbitals, not individual electrons. The systems we are interested in for fluorescence typically have singlet states or rarely triplet states. There are multiple quantized energy levels ($S_0, S_i \ldots$) these molecular orbital states can have. We can use a photon with energy matching the difference between the molecular orbital's ground state S_0 and one of its higher energy states S_i to promote the molecular orbital to this excited state. This process is called absorption. The molecule will then typically very quickly release energy as vibration and "relax" to its lowest energy excited state. A molecule in an excited state S_i stays there a finite amount of time before it transitions back to its ground state. If this transition involves emission of a photon, it is a radiative transition. Fluorescence is the radiative transition between singlet states. In fluorescence, the emissive state is typically the lowest excited singlet state, a principle called Kasha's Rule. It is also possible for the fluorophore to lose the energy via a non-radiative process, one not involving the emission of light. Such non-radiative decays may be the result of collisions and heat dissipation. The absorbed energy may be used to alter its rotational and vibrational states. This is why the energy of the photon being absorbed by the molecule is not necessarily the same as the energy of the photon being emitted by the molecule. The energy difference between the absorbed and emitted photons is called its Stokes' Shift. This photon is emitted in an arbitrary direction as fluorescence is independent of the direction of the absorbed photon. It is conceptually wrong to think of the emitted photon in some way being related to the photon absorbed; it is merely the result of the molecule releasing excess energy. In fact, the excess energy may not even come from absorbing a photon; it can also come from a chemical reaction (chemiluminescence), electric

(current/electroluminescence), or heat (kT) interactions. The molecule has no recollection of how it got into an excited state.

An excited molecule stays in its excited state for a finite time. The average time a molecule spends in the excited state S_1 before radiatively returning to the ground state S_0 is called its "fluorescence lifetime." A single fluorophore when excited multiple times will stay excited for a different time in each excitation cycle. Typical fluorescence experiments involve the excitation of an enormous number of molecules and the emission of many photons. Therefore, the deactivation of the excited state is considered a statistical process. Molecules decay from the excited state at a rate $\Gamma + K_{nr}$, where Γ is the radiative rate and K_{nr} is the non-radiative rate. This leads to an exponential decay for the population of excited molecules. In general, the number of molecules in the excited state *N(t)* can be described as [20]

$$N(t) = N_0 e^{-\frac{t}{\tau}}, \tag{18}$$

where $\tau = (\Gamma + K_{nr})^{-1}$ is defined as the fluorescence lifetime and N_0 is the initial number of molecules excited. At a time $t = \tau = (\Gamma + K_{nr})^{-1}$, the number of molecules remaining in the excited state will be $N(\tau) = N_0 e^{-1} = 0.368 N_0$ or 36.8% of N_0.

Since fluorescence intensity is directly proportional to the number of excited molecules, the time-dependent fluorescence intensity can also be described as an exponential decay,

$$I(t) = I_0 e^{-t/\tau}. \tag{19}$$

Presently, the most common technique used to measure fluorescence lifetime is a technique called "Time-Correlated Single Photon Counting" (TCSPC)[25]. Generally, a sample of the fluorophore is excited with a pulsed laser light source at a high repetition rate, typically in the range of megahertz. The first photon that reaches the detector after each excitation pulse is registered by the detector. Due to the high repetition rate of the laser, a substantial number of photons are accumulated. The

measured intensity decay is deconvoluted with the lamp function, which has a width of picosecond to nanoseconds, using nonlinear least-square fit analysis[26-29].

3.2 Measuring Emission

Figure 3 shows a general schematic of a typical spectrofluorometer. This is a right-angle instrument configuration where the excitation line and emission detection line form a 90° angle (so-called square geometry). Sometimes a single line detection configuration is utilized called "L-format" configurations when only the left or right channel is used.

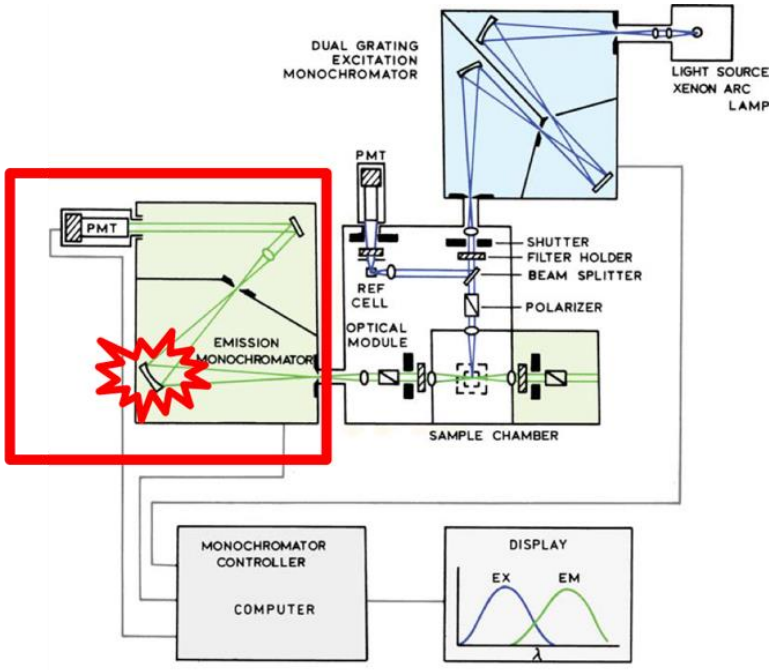

Figure 3: Schematic diagram of a spectrofluorometer[30]

The full spectrum of light from the excitation lamp (typically Xenon) goes to the excitation monochromator where an appropriate wavelength can usually be selected using a double diffraction grating. One needs to remember that selecting a given wavelength from a monochromator means selecting a bandwidth of wavelengths at each step. Depending on the selected slits (or slit width settings) the bandwidth can typically vary from 1nm – 20 nm. An

excitation beam passes through the polarizer and is focused on the sample (typically in a cuvette). The sample's fluorescence is collected through a lens, passes the emission polarizer, and is then focused on a diffraction grating in the emission monochromator. The monochromator scans the user selected wavelength range through the emission spectrum. Most diffraction grating-based monochromators select the bandwidth in nanometers (e.g., 10 nm), which is kept constant through the entire scan. A prism-based monochromator may select the bandwidth in an energy scale (e.g., 500 kK (kiloKaiser)) that is kept constant throughout the scan. The light from the monochromator is focused on the detector, which is typically a photomultiplier tube (PMT). The signal from the PMT is measured at each wavelength point and graphed as an emission spectrum by an electronic data collection system. Typical measurements are done by scanning the emission monochromator with a fixed excitation wavelength. This is called the emission spectrum. Another possibility is to scan the wavelength on the excitation monochromator with a fixed observation wavelength of the emission monochromator. The observation wavelength should be within the emission spectrum of the sample. This is called the excitation spectrum. Sometimes we can also use a synchronous scan where both monochromators are scanned with a fixed wavelength separation, i.e., excitation at λ and emission at $\lambda+\Delta\lambda$.

3.3 Fluorescence Anisotropy

Sharing the same concept with linear dichroism concerning the absorption transition moment, fluorescence anisotropy is a consequence of the linear transition moments associated with the absorption and emission processes. For practically all organic molecules that have a fixed linear transition moment within their molecular structure, the absorption process is governed by the principle of photoselection. The probability for a given molecule to absorb a photon is proportional to $cos^2\beta$ where β is the angle formed between the direction of the molecule's transition moment

and the plane of polarization for the photon. This means molecules excited by polarized light will be selected to form a non-isotropic distribution of excited molecules. Consequently, the resulting fluorescence emission will be non-isotropic as well. The extent of polarized emission light will depend on the relative orientation between the absorption transition moment and the emission transition moment at its instant of emission. For colinear transition moments, the emitted polarization is the highest. During the fluorophore's fluorescence lifetime, it may change its orientation, and thus this will affect the distribution of photoselected molecules and yield a lower polarization. Therefore, by measuring the polarized emission spectra of the sample, fluorescence anisotropy provides critical information such as molecular mobility, molecular size, and solvent (environmental) viscosity. Very importantly, an anisotropy measurement is a ratio-metric measurement that is independent of the excitation lamp intensity. In addition, the measured anisotropy will depend on the excitation wavelength used, and thus the anisotropy measured as a function of excitation wavelength will bring forth information about the relative orientation of transition moments for different absorption transitions.

Emission anisotropy for an isotropic system with cylindrical symmetry can be defined as

$$r = \frac{I_{\parallel} - I_{\perp}}{I_{\parallel} + 2I_{\perp}}, \tag{20}$$

where $I_{\parallel}$ and $I_{\perp}$ are the two corresponding polarized emissions that have the polarization of the observed intensities parallel and perpendicular to the excitation light's polarization. Theoretically, the limit of anisotropy for an isotropic system is -0.2 to 0.4[20]. Those limiting values can only be exceeded in systems that satisfy the two following conditions: the fluorophore must have co-linear absorption and emission transition moments, and also, the system must be completely frozen (no molecular rotation between absorption and emission processes). In the case when the absorption and the emission transition moments form an angle α, the anisotropy of the system is[20]

$$r = 0.4\left(\frac{3\,cos^2\,\alpha - 1}{2}\right). \quad (21)$$

The two extreme values of α are 0° and 90°, which make the limiting anisotropies for a fluorophore in a solution +0.4 and -0.2 respectively. At an angle $\alpha = 54.7°$, the system's anisotropy is zero.

3.4 Measuring Anisotropy

Fluorescence anisotropy involves measuring the difference between two orthogonally polarized light emission intensities. One of the common issues of fluorescence anisotropy measurements is that most optical detection systems respond differently to parallel and perpendicular polarizations of light. There are many reasons for this. First, the inherent detector sensitivity to light's polarization can be different. Second, optics such as reflecting mirrors, gratings, and lenses will contribute to the transmitted/transferred light's polarization. Each element will polarize/depolarize their light differently. For those reasons, measuring the precise value of anisotropy is not a simple task. A solution to this problem is to estimate a so-called "G-Factor"- a parameter which tells how much an optical detection system contributes/distorts parallel and perpendicular light polarization. This parameter can be strongly wavelength dependent and must frequently be checked during polarization measurements.

Depending on the experimental configuration and setup, there are different approaches to evaluate the G-Factor. In the simplest case of square geometry as in Figure 3, the observed polarized light is precisely at a 90° angle about the excitation light's polarization. It is most convenient to use a horizontal polarization for excitation light, typically done by rotating the excitation polarization to 90°. Vertical polarization is typically referred to as 0°. Since the distribution of excited molecules is governed by the photo-selection rule[20], a horizontal excitation on the y-axis must yield a

symmetrical distribution when observed along the x-direction. Both *z* and *y* polarized emission components, $I_{\parallel}$ and $I_{\perp}$ respectively, must be equal. Thus $I_{\parallel} = I_{\perp}$.

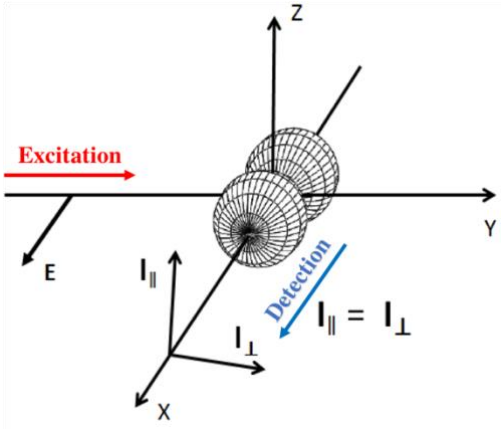

Figure 4: Distribution of the excited transition moments.

If we define the G-Factor as $G = I_{\parallel}/I_{\perp}$, the ratio $I_{\parallel}//I_{\perp}$ should be equal to one. Any deviation from the value of one is thus the result of a detection polarization bias and should be corrected. The corrected anisotropy in square geometry can be then calculated as

$$r = \frac{I_V - G * I_H}{I_V + 2G * I_H}, \tag{22}$$

where I_V and I_H are the two emission intensity components of the fluorophore corresponding to the polarization orientation of excitation and detector observation as vertical/vertical and vertical/horizontal.

In Figure 5, we illustrate the measurement of the G-Factor of the K2 spectrophotometer (ISS Inc.). Figure 5A, including four graphs on the left, shows the two components of emission spectra with the same horizontal excitation and vertical/horizontal observation for the four selected fluorophores, which are labeled as 2AP, BBO, C135, and Ru. The polarized emission spectra varied significantly across each sample and within each fluorophore itself. Notice that since the G-Factor is ratio-metric, the concentrations of these four samples were irrelevant. We used the

concentrations that provide significant intensity without troubling us with the inner filter effect. The calculated G-factors $G = \frac{I_{||}}{I_{\perp}} = \frac{HV}{HH}$ for different dyes were presented in Figure 5B (4 graphs on the right).

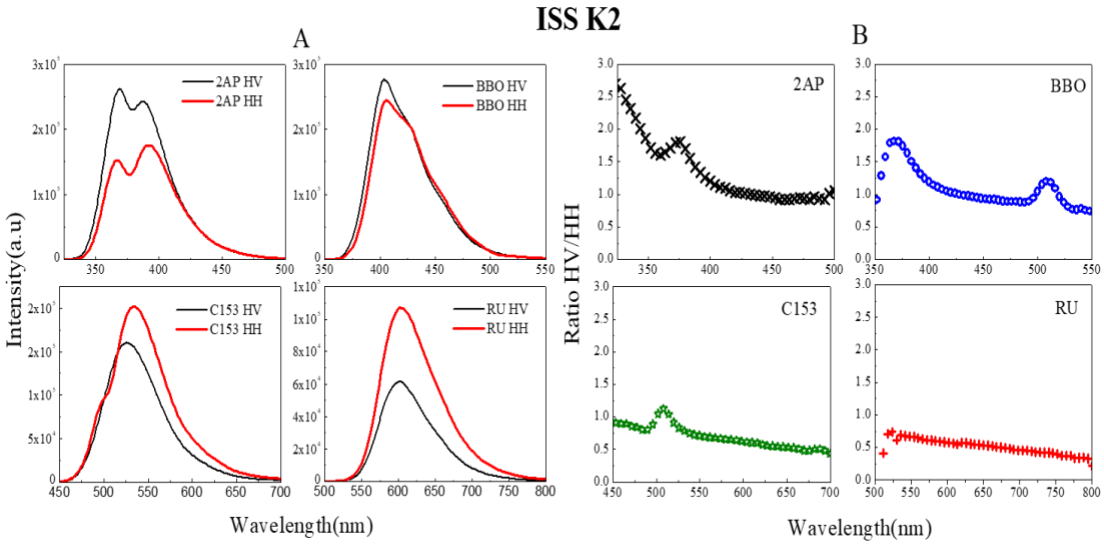

Figure 5: G-Factor measurement for the ISS K2 spectrophotometer with four dyes.

Figure 6 shows all the four previously measured G-Factors from Figure 5 in one graph spanning the entire working spectral range. The G-Factors for different fluorophores must overlay well along their overlapping emissions since the G-Factor is the instrument characteristic and cannot depend on the used fluorophores. It is expected to observe a significant statistical variation on each fluorophore's edge where their emission spectrum's signal is low.

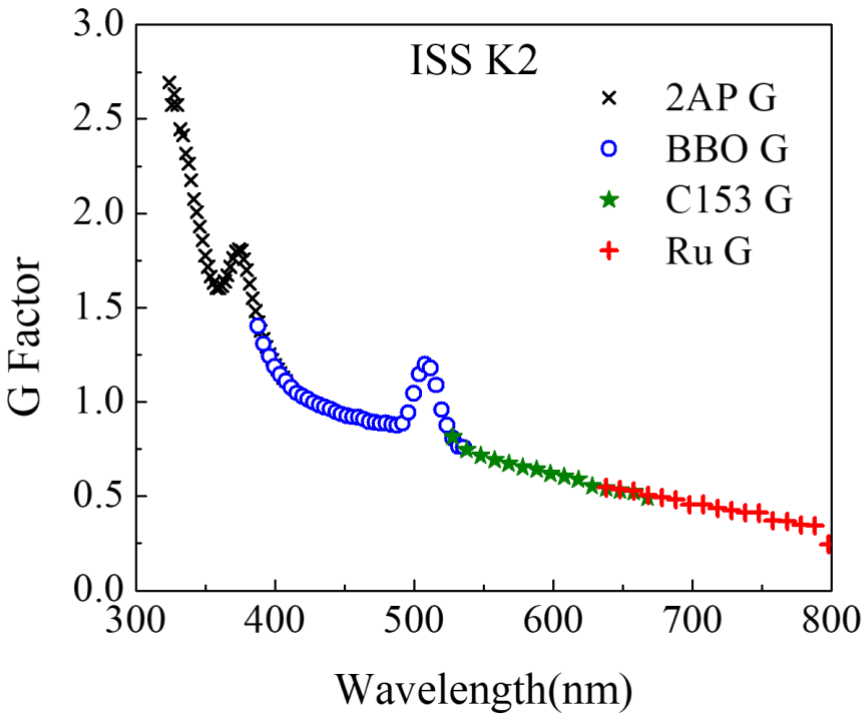

Figure 6: The G-Factor of ISS K2 spectrophotometer.

Chapter 4 Materials, Methods and Spectroscopy Measurements

4.1 Materials

4.1.1 Porphyrin Dimer

Porphyrins are an important class of organic molecules, whose derivatives can be found in many forms in nature and living species. A porphyrin consists of four pyrrole subunits connected via methine bridges (Figure 7A). Adding a metal atom or ion into the porphyrin core center makes it a metalloporphyrin. Derivatives of metalloporphyrins serve as the fundamental building blocks for many proteins in biological systems. The diversity ranges from oxygen's transfer and storage molecules such as hemoglobin (Figure 7B) and myoglobin to energy conversion in photosynthesis such as chlorophyll (Figure 7C), and even electron transfer such as cytochrome. The main diversity of metalloporphyrin functions comes from the different metal ions (iron in hemoglobin and magnesium in chlorophyll) that are coordinated in the central core of the porphyrin ring (Figure 7A). Porphyrins have also been proven to be an effective photosensitizer in PDT due to the interaction of their triplet excited state with the triplet ground state of molecular oxygen in the body. This interaction generates reactive oxygen species that function as cytotoxic agents to the surrounding tissue. The porphyrin-based drug called Photofrin® was one of the first approved photosensitizers[31,32]. Photofrin® has a weak but broad wavelength absorption maximum in the Q-bands centered at 630 nm. Excitation light used at this red wavelength can penetrate up to 5 mm into the tissue, while blue or green excitation would penetrate only a few micrometers. Photofrin® is also a useful photosensitizer because of its ability to accumulate into solid tumor sites and low toxicity to the body.

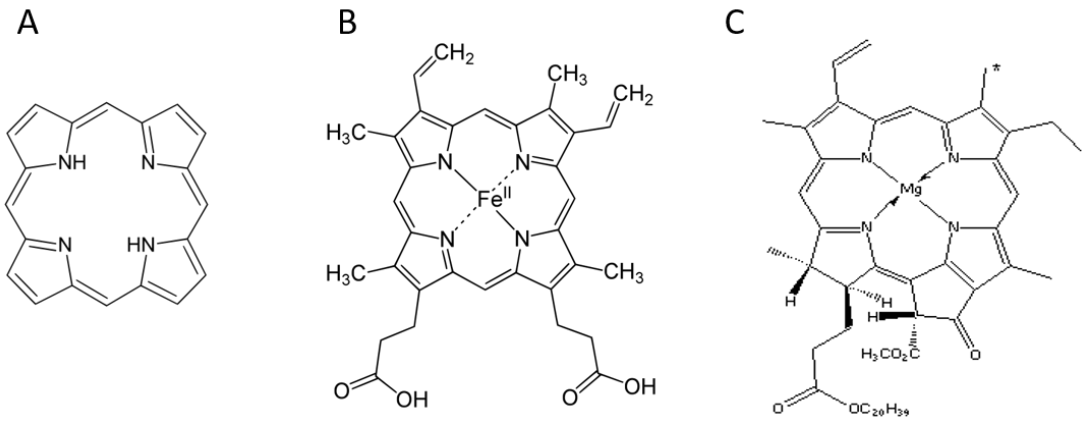

Figure 7: Porphyrin (A) and its metalloporphyrin derivatives (B and C).

Porphyrins' absorption spectrum consists of a strong transition at about 400 nm, which is due to the transition from the ground state to its second excited state (S_0 to S_2). It is named the Soret band, or sometimes, the B-band. In addition to the Soret band, there is are more, although weaker, absorption transitions beyond 550 nm, called Q-bands, which correspond to the weak transition to the first excited state (S_0 to S_1). We can use the four-orbital model of Martin Gouterman [33] to explain the two distinct absorption bands of porphyrins. According to Martin, the Soret and Q-band's absorption is the result of π–π* transitions between two HOMOs (Highest Occupied Molecular Orbital) and two LUMOs (Lowest Unoccupied Molecular Orbital), whose energy separations are dictated by the central metal atom and the substituents on the metalloporphyrin ring. Calculation of energy level suggests the HOMOs are a_{1u} and a_{2u} orbitals, while the LUMOs are a degenerate pair of e_g orbitals as shown in Figure 8a.

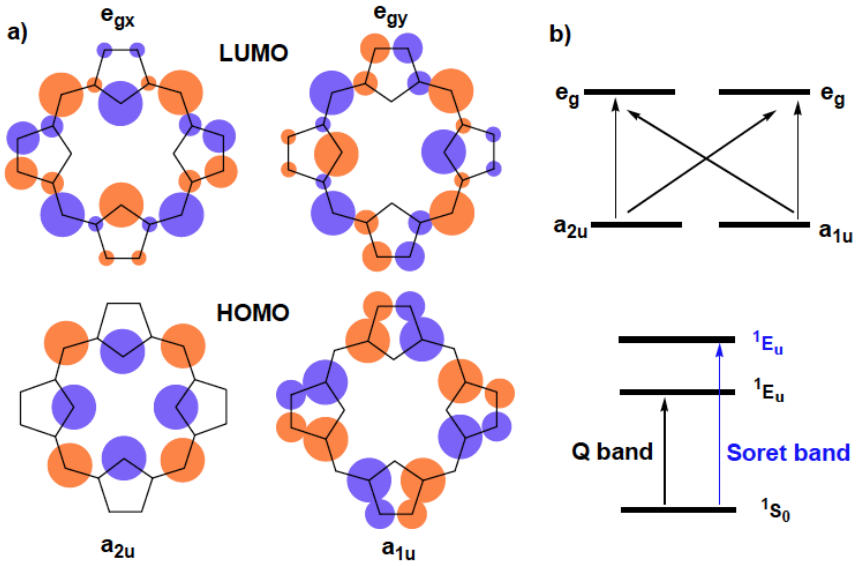

Figure 8: Porphyrin HOMOs (bottom row) and LUMOs (top row) molecular orbitals[34] (blue and orange circles represent positive and negative charges respectively).

The transitions between these orbitals are responsible for the two excited states S_1 and S_2, both of ^1E_u character. Specifically, the orbital mixing splits the two excited states into a higher energy S_2 with a greater oscillator strength, corresponding to the Soret band, and a lower energy S_1 with a weaker oscillation strength - the Q-bands (Figure 8b and Figure 9).

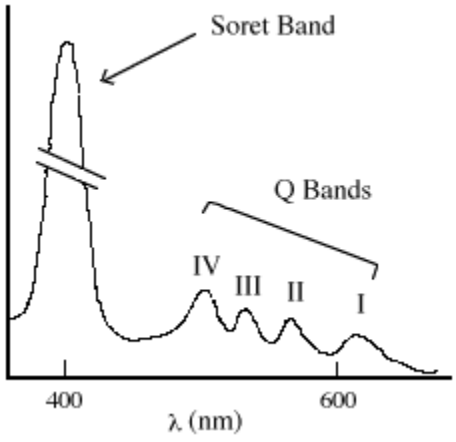

Figure 9: UV-Visible absorption spectrum of porphyrin[35].

The porphyrin derivative used in this study, porphyrin dimer (PD) was synthesized by Dr. Milan Balaz and his colleagues in 2009. The procedure of synthesizing PD was reported in literature[4]. PD's structure is shown in Figure 10, where the substituent R is the third in line and labeled as the P_2C_2-NMeI group.PD's molecular structure and purity were confirmed by MALDI-TOF (Matrix-Assisted Laser Desorption/Ionization Time-of-Flight) mass spectrometry and HPLC (High Performance Liquid Chromatography). PD is a molecular rotor that exhibits both the properties of a molecular rotor (viscometer) and a photosensitizer for PDT (Figure 10). Traditionally, the term molecular rotor describes molecules that consist of two or more parts that can undergo an internal rotary motion. This rotary motion of the molecular rotor leads to differential orientation of the rotating moieties relative to each other and thus producing a collection of conformers. In general, such a rotation is one-dimensional, and it involves changes in a single (torsional) angle. PD is a highly-symmetric conjugated organic molecule that constitutes an excellent example of a molecular rotor. The rotation of the two porphyrin units around the diyne moiety produces two distinct conformers called planar and twisted as the extremes of this rotation. Significantly, both of these conformers of PD emit at distinctly different wavelengths: the twisted /non-conjugated one at a maximum of 720 nm and the planar/conjugated one at a maximum of 780 nm. The distinct photophysical properties of these two conformers allow for a reasonably straightforward assessment of the PD's preferred conformer under a given set of conditions. Since the aggregation of PD is unlikely due to the presence of the substituent glycol-moieties on both porphyrin units, extensive studies using PD as a probe for various types of environments, including cellular, micellar, and gel-like media as well as molecular and ionic liquids have been carried out in recent years[1,2].

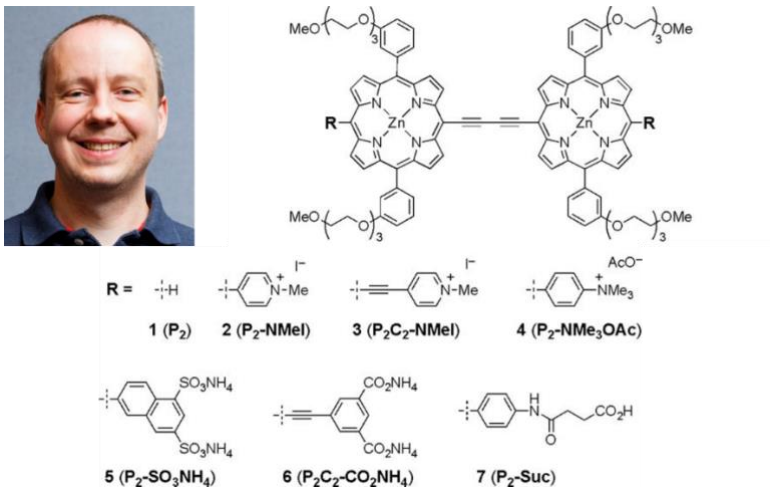

Figure 10: Dr. Milan Balaz and his PD system.

Also, PD might also be used as a sensitizer in photodynamic therapy[6,36], since its Q-bands absorption is conveniently located for activation by radiation in the red spectral range. In a typical biological system, any wavelength beyond 900 nm is absorbed by water, whereas wavelengths less than 700 nm are either scattered by macromolecules or absorbed by hemoglobin[37,38]. This leaves a small range of wavelengths from 700 nm to 900 nm, sometimes referred to as the therapeutic window, to conveniently activate the photosensitizers using red light sources. This allows us to control the activation region by light illumination alone. The benefit of localizing the oxidizing singlet oxygen is that it minimizes collateral damage around the focused position.

4.1.2 Solvents and PVA

All solvents and other materials, including polyvinyl alcohol (PVA, 130 kDa), were purchased from Sigma-Aldrich and were used as received. A 1 mM concentration stock solution of PD in dimethyl sulfoxide (DMSO) was prepared fresh before the experiments, and it was used for all spectroscopic measurements and protected from direct light exposure during storage.

4.2 Methods and Spectroscopy Measurements

4.2.1 Preparation of PVA films

PVA films were prepared according to previous literature[39]. Briefly, double distilled water (170 mL) was added to a 250-mL flask containing a magnetic stirring bar. PVA powder (30 g) was slowly added under stirring at 80ºC -90ºC, and the stirring continued for 2 hours. Bubble formation was noted during this step. The resulting homogeneous solution was allowed to cool to room temperature overnight to clear out all the bubbles.1-2 µL of 1 mM DMSO stock solution PD was added to a freshly prepared PVA solution (6.0 mL in a 20 mL glass vial) at 40ºC -50ºC. The mixture was thoroughly mixed using a glass pipette for 10-15 minutes to assure complete mixing, followed by sonication for 2-3 minutes to remove all bubbles that formed during the mixing. Next, the mixture was poured into a 2-inch diameter plastic petri dish on a flat and balanced surface and kept in a moisture-free, dark environment for 4 to 6 days to allow the film to form.

4.2.2 PVA Films Stretching/heating Procedure

PVA films with embedded PD were uniformly stretched (up to four times the original length) using a home-built stretching apparatus. In a typical experiment, a PVA film was mounted and then two dots with a distance of 0.5 cm to each other were marked near the center of the film. The temperature was monitored using an electronic hot plate with a built-in temperature controller. Also, a thermocouple was mounted closely underneath the PVA film to monitor the local temperature of the stretched region.

Figure 11: Photographs of the home-built stretching/heating instrument.

All stretchings with heat were performed at 70 ± 1°C. All films were stretched at a slow and consistent rate (0.5 cm per 20 seconds) to avoid tearing of the film. Stretching at room temperature was done at a slower rate, typically 0.5 cm per 30 seconds, to avoid fracture and loss of transparency. Figure 12 shows the photographs of PD-PVA films. The extent of stretching was calculated by taking the ratio of the final distance between the two dots at the center relative to the original distance of 0.5 cm.

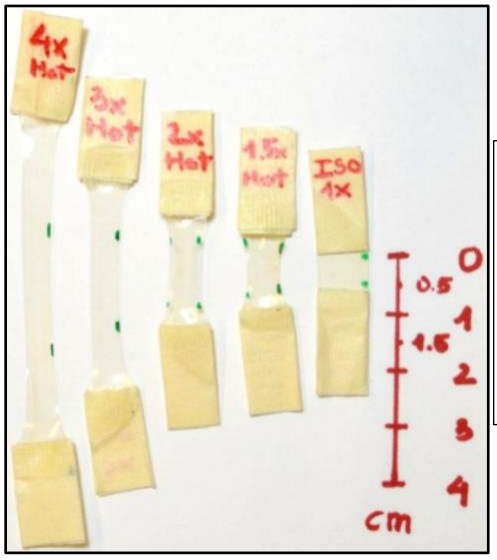

ISO 1x:	non-stretched	(0.5 +/- 0.05 cm)
1.5x:	stretched to 150%	(0.75 +/- 0.05 cm)
2x:	stretched to 200%	(1.0 +/- 0.05 cm)
3x:	stretched to 300%	(1.5 +/- 0.05 cm)
4x:	stretched to 400%	(2.0 +/- 0.05 cm)

Stretching is done at 70 ± 1°C.

Figure 12: Photographs of PD-PVA films and their lengths.

The thickness of the films (both stretched and non-stretched) was measured using an electronic caliper and with a micrometer caliper. Measurements were performed at the center of the film between the two dots. Table 1 shows the thickness of PD-PVA films as a function of stretching at 70°C

Table 1: Thickness of PD PVA film as a function of stretching at 70°C.

Extent of stretching	**length / cm**	**thickness / cm**
non-stretched	0.5 +/-0.05	0.035 +/-0.005
2 (200%)	1.0 +/-0.05	0.021 +/-0.005
3 (300%)	1.5 +/-0.05	0.018 +/-0.005
4 (400%)	2.0 +/-0.05	0.015 +/-0.005

4.2.3 Absorption and linear dichroism

The UV-Vis absorption spectra of PD in solvents were measured with a Cary 60 UV-Vis Spectrophotometer (Agilent Technologies). Linear dichroism measurement was performed using Cary 60 UV-Vis Spectrophotometer with an adapted home built PVA films holder, and a wire-grid polarizer. Two orthogonal absorption components $A_{\parallel}(\lambda)$ and $A_{\perp}(\lambda)$ for which the light polarized parallel ($\parallel$) and perpendicular ($\perp$) to the stretching direction respectively were measured. Those two components allowed us to calculate the linear dichroic ratio.

4.2.4 Fluorescence and Fluorescence anisotropy

Emission spectra were obtained using the ISS K2 spectrofluorometer (ISS Inc) with a custom-built front-face apparatus. A Xenon lamp was used as the excitation source. To select the desired excitation wavelength, the white light was passed through the excitation monochromator and additional filters as needed. Then, the selected excitation was passed through a Glan-Thomson

polarizer and further onto the sample. Fluorescence signal from the sample was collected through the lens and passed through the second Glan-Thomson polarizer before getting into the emission monochromator and finally to the detector.

The stretched PD-PVA films were mounted vertically along the stretching axis. VV, VH, HV, and HH of emission spectra correspond to the orientation (vertical/V and horizontal/H of the two Glan-Thomson polarizers that were placed between the sample and the excitation light, and between the sample and the detector, respectively. For example, VV spectra were obtained by using excitation light through a vertically (V) oriented Glan-Thomson polarizer (this gave polarization of excitation light which was parallel to the stretching axis). The light emitted from the PD-PVA film was passed through another Glan-Thomson polarizer also oriented vertically (V), thus only allowing vertical fluorescence light to come to the detector[40].

Fluorescence anisotropy of PD in PVA films was measured with the same instrumentation configuration. The correcting factor (G-Factor) for instrument have independently been determining.

4.2.5 Fluorescence Lifetime

Fluorescence lifetimes were measured on a FluoTime 300 fluorometer (PicoQuant, Inc.). Pulsed laser excitation was provided by a Supercontinuum White Laser SC-400 (Fianium, Ltd). The system generates pulses of white light with a pulse-width of about 6 ps. To selected desirable wavelength white excitation light was passed through a hybrid quartz prism and grating monochromator to choose an excitation light of 475 nm (± 5 nm). The fluorometer was equipped with an ultrafast microchannel plate MCP/PMT (Microchannel plate/Photomultiplier tube) detector from Hamamatsu and collected with the resolution set to 4 ps/channel. The fluorescence

lifetimes were measured at the magic angle condition (54.7°), and data were analyzed using the FluoFit4 program from PicoQuant, Inc (Germany) using multi-exponential fitting model

$$I(t) = \sum_i \alpha_i e^{-\frac{t}{\tau_i}}, \tag{23}$$

where α_i is the amplitude of the decay of the i^{th} component at time t and τ_i is the lifetime of the i^{th} component. The intensity weighted average lifetime (τ_{avg}) was calculated using the following equation

$$\tau_{avg} = \sum_i f_i \tau_i \text{ where } f_i = \frac{\alpha_i \tau_i}{\sum_i \alpha_i \tau_i}. \tag{24}$$

4.2.6 Percentage planar conformation

Percentage of the planar PD conformation (planar PD %) was calculated as follows[41]

$$Planar\ PD\ \% = \frac{F_{planar}^{max}}{F_{twisted}^{max} + F_{planar}^{max}} * 100, \tag{25}$$

where $F_{twisted}^{max}$ is the maximum fluorescence intensity of the twisted conformation; F_{planar}^{max} is the maximum fluorescence intensity of the planar conformation.

Chapter 5 Results and Discussion

5.1 Molecular Structure of PD's Extreme Conformations

Figure 13 illustrates the chemical structure of the conjugated zinc porphyrin dimer (PD). PD may undergo rotation around the diyne moiety, resulting in two discrete conformations. These two extreme conformations are denoted as twisted and planar, which correspond to the out-of-plane and in-plane positions of the two zinc porphyrins units. Furthermore, due to the triethylene glycol moieties on the porphyrin core and the preferred twisted orientation of the phenylene groups, PD is unlikely to form aggregates in solutions and remains as monomers[4].

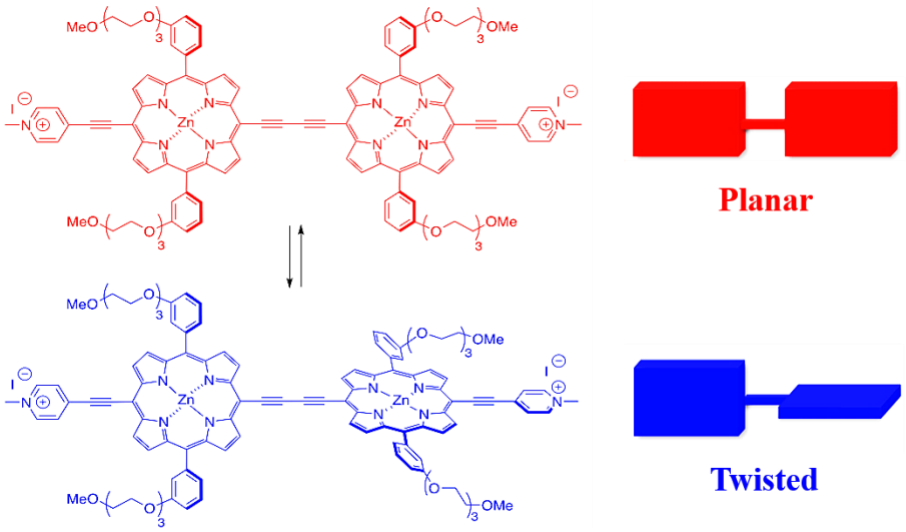

Figure 13: Chemical structure of PD's conformational extremes (planar and twisted).

5.2 Absorption of PD in Solvents and PVA

The absorptions of PD were investigated in some common solvents such as ethanol, propylene glycol, glycerol, and in PVA film (PD/PVA film). Results are shown in Figure 14. The selected solvents largely differ in viscosity, covering the range from 0.983 mPa s in ethanol to 1501 mPa s in glycerol and PVA is considered as a medium of infinitely high viscosity. In all experimental

solvents, PD exhibited a strong Soret band absorption with a maximum at 470 nm and a weaker Q band absorption with two distinct peaks at about 700 nm and 775 nm. Overall, we observed no significant differences in the Soret band absorptions of PD in various solvents, besides a slightly visible shoulder at 510 nm in PVA. The noticeable differences are present in the construction of the Q-band for different viscosity solvents. As the viscosity increases from EtOH to Propylene Glycol, to glycerol, and to PVA the longer wavelength transition of the Q-band becomes more prominent. The peak at 780 nm significantly dominates the 710 nm one in PVA, as compared to the other media.

A significant change in the fluorophore absorption spectra in different solvents is somewhat unexpected. Especially since selected solvents mainly differ in viscosity. This may indicate that solvent viscosity changes the equilibrium between twisted and planar conformations. As we increase the solvent viscosity, we are preferentially increasing the population of the planar conformation[1].

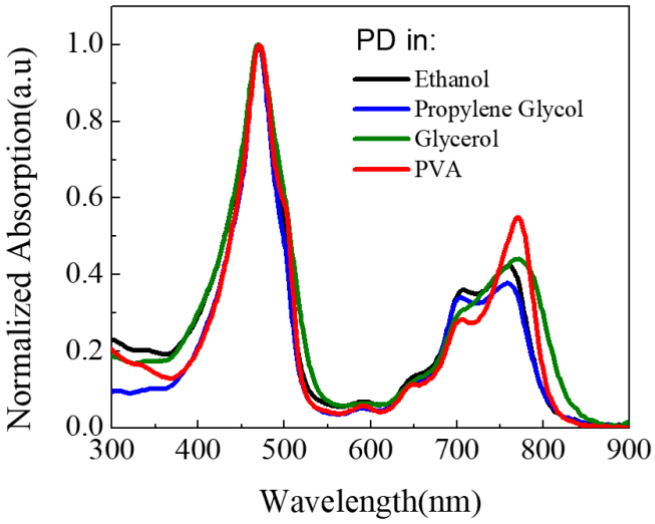

Figure 14: Absorption spectra of PD in solvents (ethanol, propylene glycol, and glycerol) and PD/PVA film.

5.3 Conformation Interconversion of PD in Different-Viscosity Media

Media's viscosity is one of the leading factors that alter the conformer ratio of PD. In all examples of different solvents, the conformations of PD were not locked. The dynamic equilibrium has been established between the planar and twisted conformers depending on the nature of the media. Upon excitation, the excited twisted conformer may emit or convert into a lower energy excited planar conformer. The efficiency of conversion to planar configuration depends on the solvent viscosity and for low viscosity media is much more efficient. In high viscosity media (such as glycerol), this process is much slower, thus leads to a ground state population of the twisted conformer[42] (Figure 15). However, if PD were to be locked in a solid-state matrix (e.g., a polymer PVA film), the interconversion between planar and twisted conformations would not be possible.

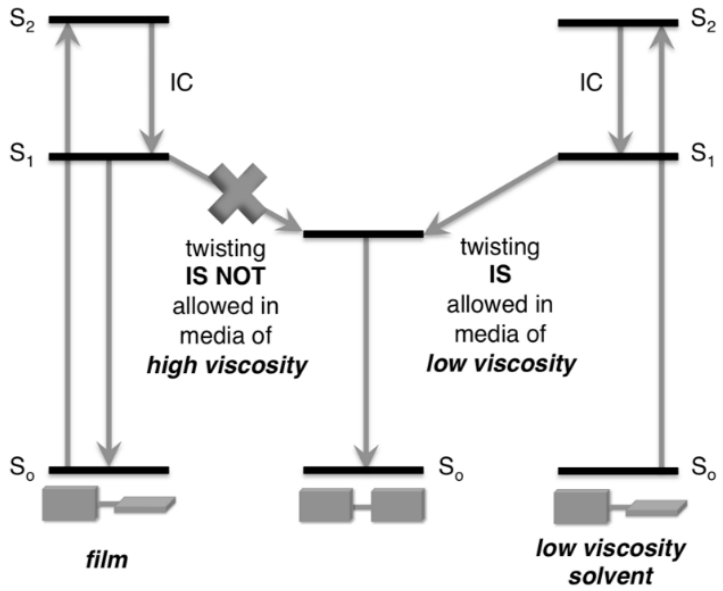

Figure 15: The allowed and non-allowed twisting cases of PD in different viscosities[41].

5.4 Polarized Absorption of PD in Stretched PVA Film and the Dichroic Ratio.

The interconversion between planar and twisted conformations of PD is strongly limited by solvent viscosity and thus in a rigid matrix interconversion would be completely prohibited. So, in a solid-state matrix (e.g., a polymer PVA film) we have a mixture of two conformations at a well-defined ratio of two populations which doesn't change with time. The absorption measurements in different viscosity solvents and solid isotropic PVA films revealed that as the viscosity increases, the equilibrium shifts toward the planar population but still a significant part of PD (>40%, judged by the ratio of the emission peaks of the twisted and planar conformers at 720 nm and 780 nm respectively) is in the twisted form.

The PVA film can easily be stretched in a uniaxial manner (stretched in one direction). Such a stretching process results in the polymer chains aligned along the stretching direction. This is a very effective approach to align elongated or/and planar molecules along the stretched axis. The polymer can be stretched at an ambient or elevated temperature. We hypothesized that stretching PVA films at room temperature where the polymer is flexible but rigid will result only in PD molecules' orientation. However, stretching at an elevated temperature (>70^{o}C) we increase the film's plasticity and promote the transition of PD molecules to a planar conformation as well. Since below 100^{o}C, PVA polymer still exhibits solid state properties, so we expected that we will be able to lock the planar conformation in the polymer.

To test this hypothesis, we did the following:

1. Measured absorption of PD in isotropic film.
2. Measured absorption of PD in isotropic film heated to about 80^{o}C.
3. Measured absorption of PD in the cold stretched PVA film.
4. Measured absorption of PD in stretched PVA at an elevated temperature (about 80^{o}C).

In Figure 16 are shown the measured absorption for an isotropic PVA film doped with PD before heating and after heating to about 80°C. The film was heated to 80°C and held at this temperature for three minutes. It was then cooled to room temperature, and its absorption was measured using an Agilent Spectrophotometer Cary 60 UV-VIS. It is clear the change in absorption is small, but it indicates a slightly more planar form.

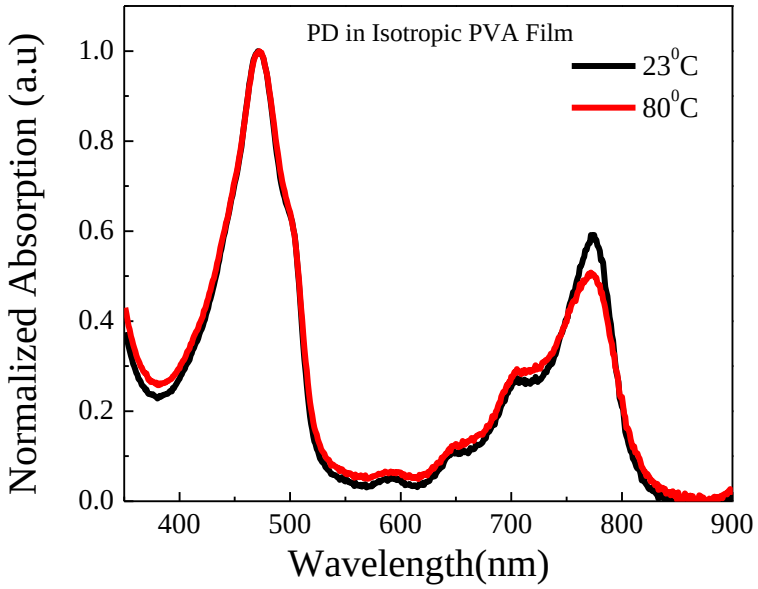

Figure 16 Absorption of isotropic PD/PVA at 23°C and 80°C.

For comparison, in Figure 17, the absorption spectra of the heated solution of PD in glycerol are shown. In this case, the measured change is minimal even with heating multiple times.

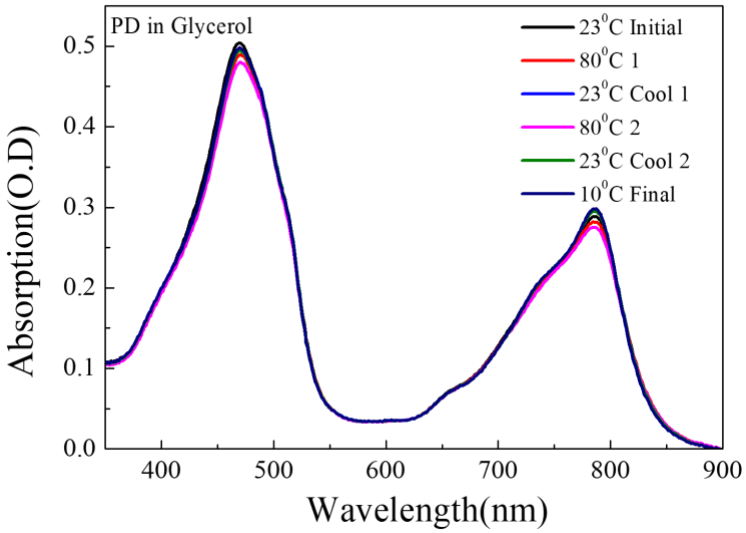

Figure 17: Absorption of PD in glycerol at 23°C and 80°C.

Next, we took a PD containing PVA film and stretched it 3-fold in ambient temperature as well as when heated to about 80°C. For stretching, we used the instrumentation as described in Figure 11. The stretching procedure typically takes about 2-3 minutes when the stretched film was cooled and measured at room temperature. Figure 18 (left) shows the parallel and perpendicular absorption components for the cold-stretched PVA 3-fold. 3-fold stretching is the maximum stretching that can be achieved at room temperature without breaking the film. The parallel and perpendicular absorption components are different, and thus the dichroic ratio ($R_d = A_{\parallel}/A_{\perp}$) is essential and indicates the good alignment of the molecules.

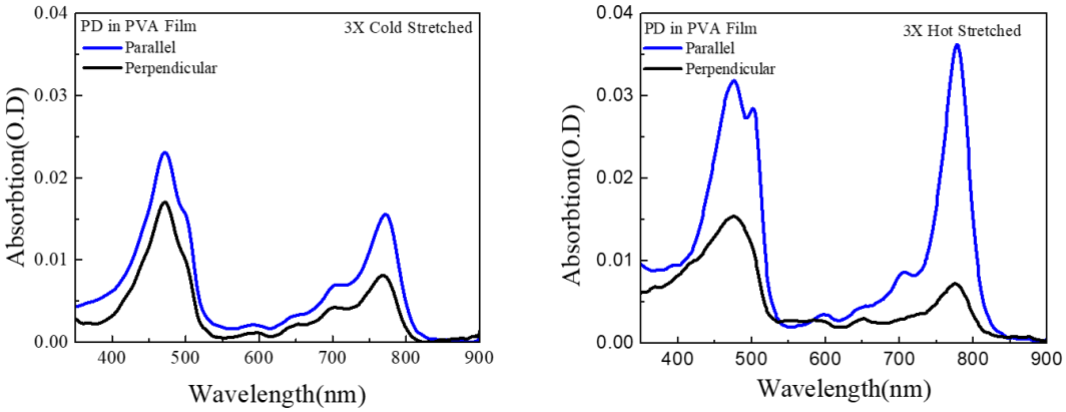

Figure 18: Absorption components of PD in 3x stretched PVA films at 23°C and 80°C.

Figure 18 (right) shows the measured parallel and perpendicular absorption components for three times stretched PVA film containing PD at an elevated temperature (~80°C). Even if the stretching ratio at room temperature and 80°C are the same, the measured absorption components (parallel and perpendicular) are drastically different. We could expect the molecular orientations to be similar, but not identical. The measured dichroic ratios (R_d) are shown in Figure 19. For the heated film, the dichroic ratio at a longer wavelength is much higher, and the measured spectral profiles for the parallel and perpendicular component are very different.

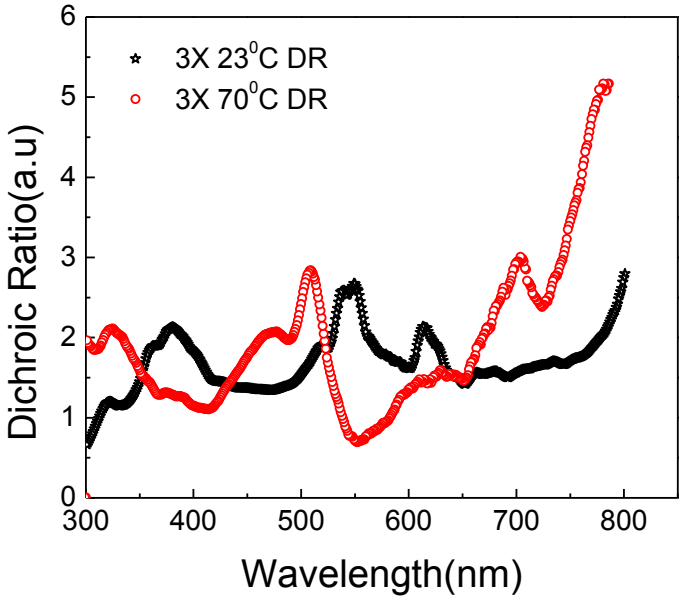

Figure 19: Dichroic ratio in 3X stretched PVA at 23°C and 80°C.

When heated, a PVA film can be easily stretched 4-fold. At this level of stretching, molecular orientation approaches maximum. In other words, further stretching does not improve the measured dichroism. Figure 20 presents the measured absorption components for a 4-fold stretched film. The open stars show the calculated LD. The Dichroic Ratio R_d reaches a value of about six at the long-wavelength range, thus indicating that the long-wavelength transition at about 780 nm is polarized along the long molecular axis.

Upon stretching up to the breaking point of the PD/PVA film (approximately 4-5 times its original length), we probably achieve almost maximal orientation of the PD molecules. It is obvious such a complex molecule would have multiple transition dipole moments. In the case of planar conformation, we can assume the strongest transitions will be located in the molecular plane that consists the *y* and *z* axes. This allows us to calculate the orientation parameters, K_y and K_z, that is defined by Michell Thulstrup as the orientation factors along the *y* and *z* axes and position of the molecule in the Orientational Triangle[18]. In Figure 20 right, we present the Orientational Triangle

with the green squares indicate the position of the planar PD's structure-like molecules. In contrast, in the twisted form, the molecule is not planar, and we can expect significant contributions from both components that are orthogonal to the long molecular axis. The calculated orientation parameters K_y and K_z place the molecule far from the orientation of the planar form.

The presented complex character of the dichroic ratio in Figure 20 (left) indicates the presence of multiple, differently-oriented absorption transition moments. It is clear the long wavelength transition in the Q-bands (about 780 nm and above) oriented along a long molecular axis. A quick drop of the dichroic ratio when moving toward the shorter wavelengths indicates that the second transition in the Q-bands has very different (almost orthogonal) orientation. The Soret band presents an even more complex character. Probably it is a complex mixture of transitions that have different orientations. This is perhaps due to different contributions of the parallel and perpendicular transitions as referred to along the long molecular axis, with very significant contributions from transitions oriented perpendicular to the long molecular axis. These are likely complex transitions associated with the inner porphyrin ring. This is likely because the dichroic ratio is only about two, which is typical for two equally distributed orthogonal transitions, where one is parallel to the long axis, and one is orthogonal. Interestingly, at the long side of the Soret band, at about 500 nm, we observe a significant increase in R_d. In this spectral range, we also can see a significant peak in the parallel absorption component. This peak in the 500 nm range is typically not visible in isotropic solutions. This is a transition oriented along the long molecular axis. In the 470 nm-480 nm range, we can see a dip in the dichroic ratio, thus indicating a dominant contribution of transitions orthogonal to the long molecular axis, as well as orthogonal to the long wavelength absorption transitions. Interestingly enough, this range (470 – 480 nm) is frequently used for PD excitation when using it as viscosity sensor. It offers a good extinction coefficient,

(better than Q-bands) but it is not the maximum of the Soret absorption band. The simple justification previously has been that such excitation offers the best dynamic range for sensing. This dichroism analysis indicates that when using 470 – 480 nm excitation wavelength, we will excite transition moments that are predominantly orthogonal to the long-wavelength absorption transition.

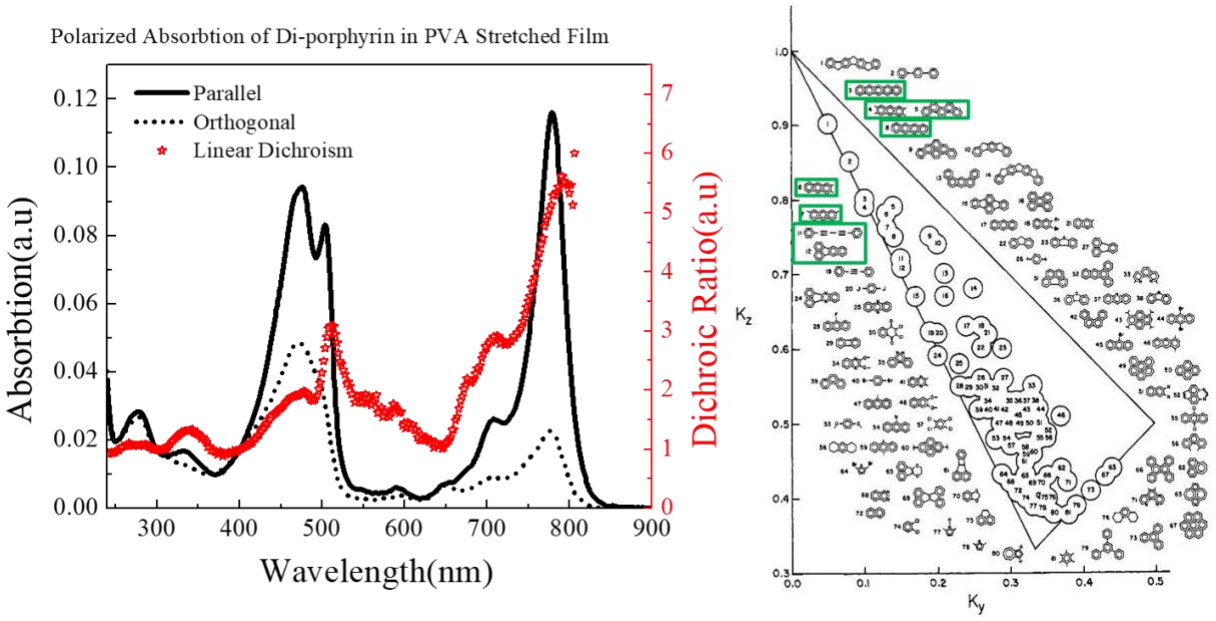

Figure 20: Dichroism ratio of PD in 4x stretched PVA and Thulstrup's orientation triangle.

5.5 Emission of the PD's extreme conformations

Previous studies showed that the twisted and planar conformers exhibit distinct emission maxima at 710 nm and 780 nm respectively[1,2]. Specifically, the emission of PD in low viscosity solutions was dominated by the lower-energy planar conformation. In contrast, the emission of the less-stable, twisted conformer could be observed at a higher viscosity solvent or solid matrix. All previous studies were done using 470 nm - 480 nm excitation range. As indicated in the previous section (Figure 20), these excitation wavelengths dominantly excite orthogonally oriented transitions as compared to the long wavelength absorption transition (780 nm).

In this part, we tested how the measured emission depends on the excitation wavelength. The goal is to establish if different values of measured dichroism would correspond to different conformers. For this, we selected wavelengths that correspond to different values of measured dichroism. The wavelengths we used were:

‣475 nm – this is the typical wavelength used for this system by other researchers. Also, this wavelength corresponds to a low value of dichroism in the Soret band. We expect this wavelength to excite an orthogonal transition that probably corresponds to the twisted form.

‣430 nm – This wavelength corresponds to a low value of dichroism (similar to 475 nm) and is positioned on another side of the Soret band.

‣510 nm – Corresponds to the very high dichroism in the long-wavelength edge of the Soret band. We expect this excitation to excite the long-wavelength transition predominantly.

‣705 nm – This is a Q-band transition that very probably is a transition associated with the twisted form. The dichroism shows a definite dip.

‣730 nm – These are long-wavelength transitions within the Q-band that dominantly correspond to the planar form.

We hypothesize that when exciting a twisted form of PD, it will undergo a conformational change (rotation from twisted to planar). When using a low viscosity solvent, the effect will be dramatic, but as we will increase viscosity, the transition will be hindered. So, for low viscosity, we should observe emission predominantly from the planar form, and as we increase the viscosity, we should see a more significant presence of twisted form in the emission spectrum. Importantly, when

exciting the transitions oriented along the long wavelength absorption transition (the long molecular axis) that correspond to planar form, we should not see emission from the twisted form. Figure 21 shows measured emission spectra for three solvents that have very different viscosities (ethanol, propylene glycol, and glycerol) using different excitation wavelengths. As expected in the case of ethanol (EtOH), the maximum emission is observed at about 790 nm independently of excitation wavelength. For 475 nm and 430 nm, we can observe a small increase at the short wavelength emission part (a bump at about 720 nm). Moving to PG, which has intermediate viscosity, the 475 nm excitation results in a significant bump at 720 nm showing significant emission contribution from the twisted form. The 705 nm excitation shows dominant emission from the twisted form. However, 510 nm is clearly showing pure emission of planar form only.

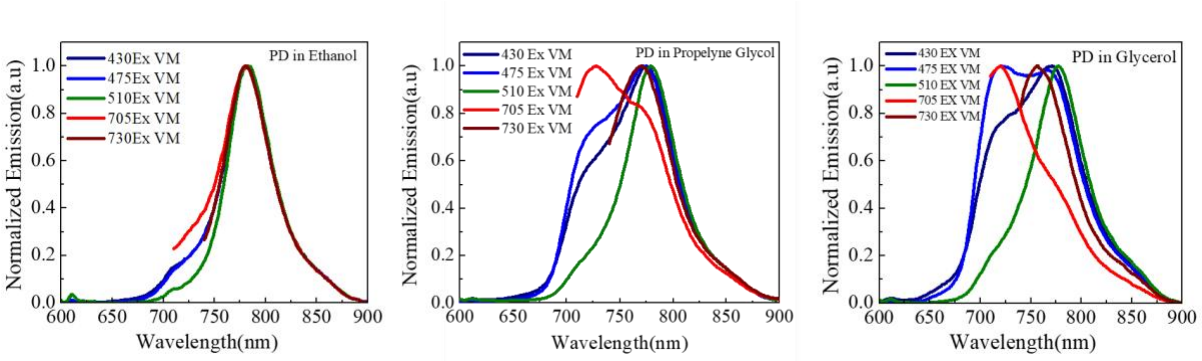

Figure 21: PD's emissions in different viscosity solvents.

Glycerol is a very viscous solvent (~1100 cP), and in this case, 475 nm excitation results in emission that is equally contributed to the porphyrin's twisted and planar forms. The emission spectrum with 705 nm excitation is the emission of only twisted form. However, again 510 nm excitation shows the only emission of planar form.

From the steady-state emission measurements, we can clearly assign emission spectra associated with the twisted and planar conformations. These are distinct emissions of two the conformers presented in Figure 22. From the measured emission spectra with different excitation, we can

predict that to study the micro-viscosity (speed of rotation) we should excite the twisted form and observe the transition to a planar form. From Figure 21 excitation wavelength in the range of 705 nm will dominantly excite the twisted form. The inconvenience with this excitation is that it is very close to emission and the extinction coefficient is rather low. The next convenient excitation is 475 nm that is far from emission range and for which PD has significant absorption. In all earlier studies[2,5,43], various researchers have been using excitation from 470 nm -480 nm range that was selected by simple trial-and-error. This study shows a rational explanation why this excitation wavelength (from 470 nm – 480 nm range) gives good results.

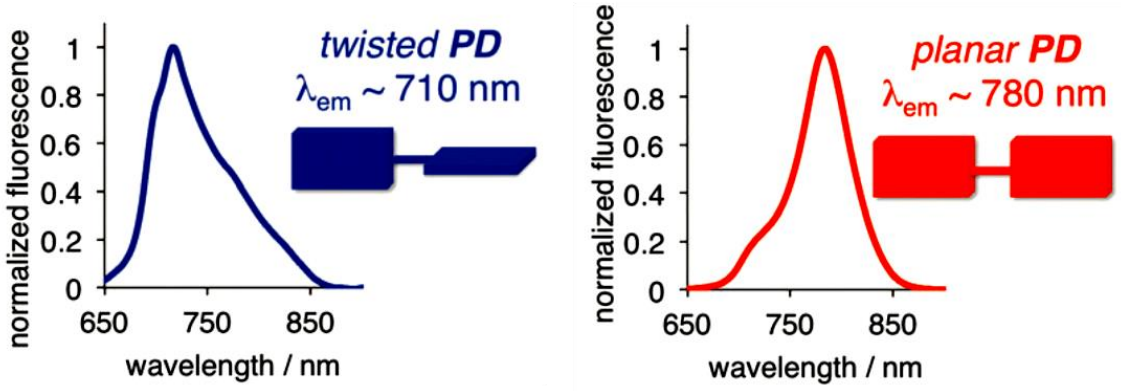

Figure 22: Emission spectra of the two-extreme conformations[41].

We also measured the emission spectra in PVA films (isotropic and stretched) using 475 nm and 510 nm excitations. In this case we should not observe the transition from twisted to planar form. In Figure 23, we present the emission spectra for the isotropic (left) and four times stretched film (right). For isotropic film, 475 nm excitation presents a dominant presence of the twisted form and 510 nm clearly planar. In the 4x stretched film, the contribution from the twisted form drops drastically. This is consistent with our previous observation that stretching and heating the film is forcing PD molecules to a planar conformation. Obviously 510 nm excitation results now in pure planar form's emission.

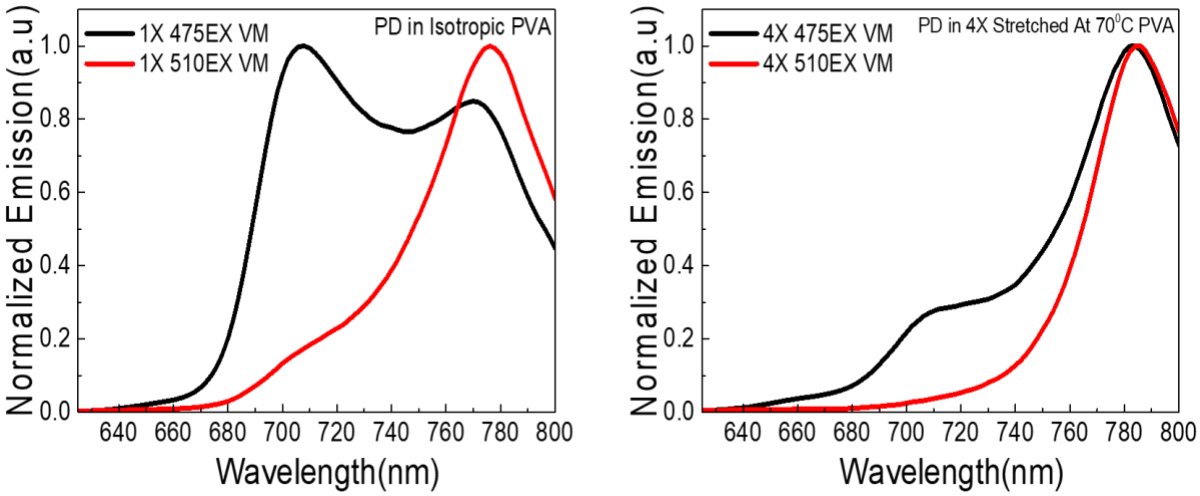

Figure 23: Normalized emission of PD in isotropic and stretched PVA films.

5.6 Mechanical force induce conformational change of PD

Overall, the results from this study revealed that a mechanical force with heating could be used to modulate the conformational equilibrium and optical properties of PD. Figure 24 is a summary of the effect of stretching at an elevated temperature and induction of PD's conformational change starting predominantly from a twisted to a planar conformation. Importantly, the increase in the planar conformation comes at the expense of the twisted conformation (Figure 24A, C) regardless of excitation wavelength, as long as the twisted conformation of PD can be excited. At 475 nm excitation where a significant part of twisted conformation is being excited, the stretching shows a maximum change. This insight provides a viable strategy for inducing desirable functionalities with potential applications in material science, sensing, and catalysis.

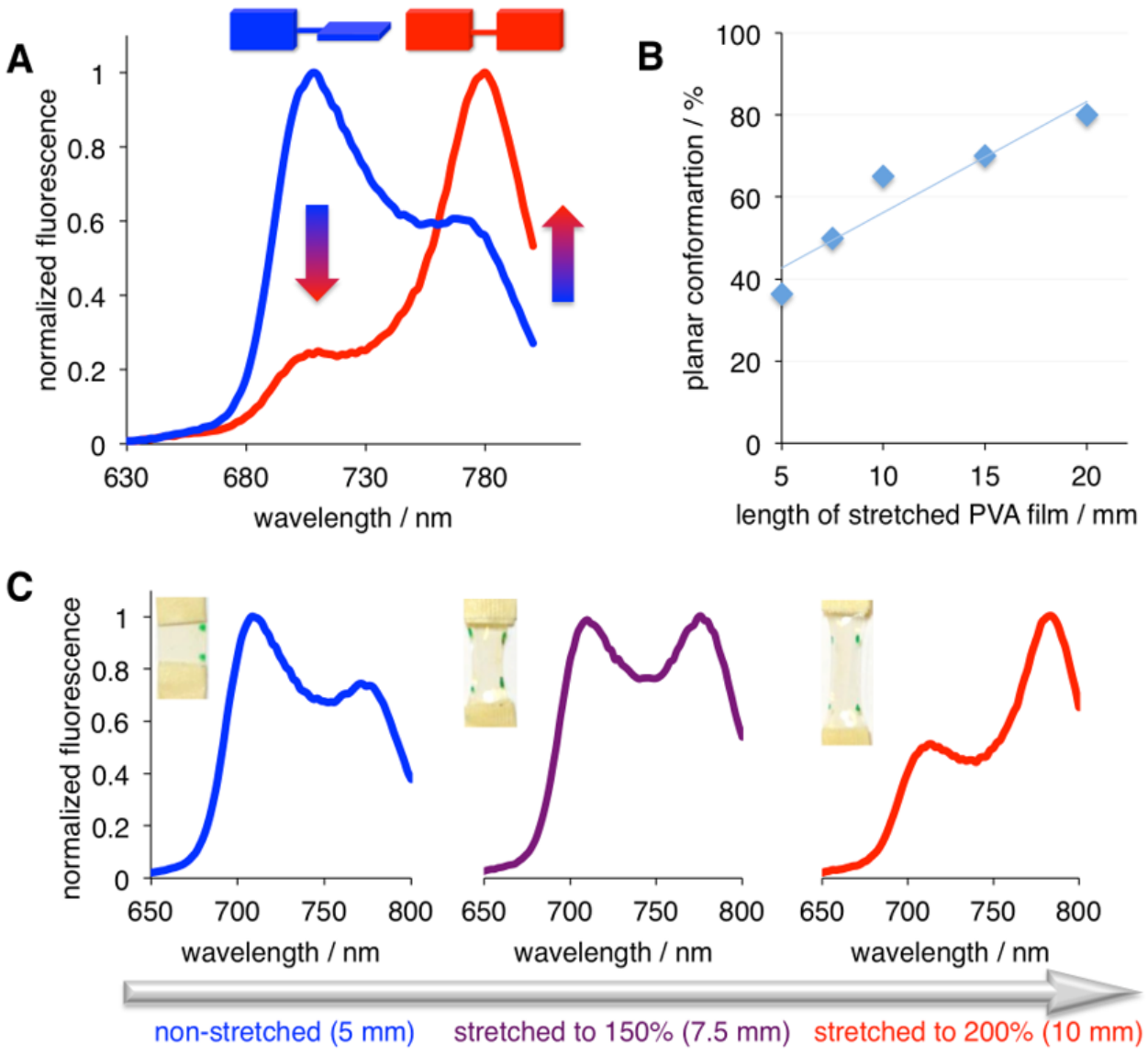

Figure 24: Thermally assisted mechanical force on the conformational change of PD[41](A) Emission spectra of PD in non-stretched (blue) and maximally stretched (4x) (red) when excited at 475 nm. (B) Planar conformation % of PD as a function of stretching; 5 mm corresponds to the non-stretched film and 20 mm to 4x stretched film. (C) The stretching-induced conformational transition from twisted (λ_{max} EM = 710 nm) to planar (λ_{max} EM = 780 nm) PD; λ_{ex} = 475 nm. The dots on the PVA films indicate the extent of stretching.

5.7 Lifetime in PVA ISO vs. Stretched

The steady-state data (both linear dichroism and fluorescence) indicates that PD exists in two conformers. Depending on the excitation wavelength, we can preferentially select one of the conformers. The steady-state measurements reveal the population of two conformers but do not expose any information about a conformational change. To test if the conformational change happens (or may happen) during its excited state lifetime we employed a time-resolved approach. The questions we asked were:

‣How do we detect the dynamics of conformational changes?

‣Does a conformational change happen in the PD system?

If the conformational change happens in the excited state, then the PD molecule can serve as a true microviscosity sensor where the measured emission spectrum will reflect the viscosity of the local system. For example, if we excite in the twisted form and observe emission of the planar form, then the amount of emission will depend on the fraction of molecules that are capable of switching from the twisted conformation to a planar one during its fluorescence lifetime. So, for low viscosity environments, we will see a high contribution of planar molecules' emission while for high viscosity environments a much lower fraction.

The last piece of information we wanted to extract would be the fluorescence lifetime of each conformation. We utilized four excitations - 430, 475, 510 and 730 nm with the PD molecule embedded into a PVA film. In this system, we do not expect a conformational change to occur. The measured fluorescence lifetimes with two observations 710 nm and 780 nm will correspond to the fluorescence lifetimes of twisted and planar forms, respectively.

Previous results indicated that while the 430 nm excitation excited both conformers, the 475 nm and 510 nm preferably excited the twisted form and the planar form, respectively. We employed 730 nm excitation to excite the planar conformation only, however, it is impossible to have an excitation where only the twisted form is excited. For each excitation, except 730 nm, we observed at both 720 nm and 780 nm where the twisted and planar forms emit respectively. Results are shown in Table 2.

Table 2: Fluorescence lifetime of PD in PVA film.

PVA	Excitation (nm)	Observation (nm)	α_1 (%)	α_2 (%)	α_3 (%)	τ_1 (ns)	τ_2 (ns)	τ_3 (ns)	$<\tau_\alpha>$ (ns)
ISO	430	720	0.44	0.43	0.13	1.75	1.18	0.13	1.29
		780	0.35	0.52	0.13	1.25	0.81	0.06	0.87
4X		720	0.25	0.63	0.12	1.95	1.23	0.22	1.29
		780	-	0.69	0.31	-	1.02	0.61	0.89

PVA	Excitation (nm)	Observation (nm)	α_1 (%)	α_2 (%)	α_3 (%)	τ_1 (ns)	τ_2 (ns)	τ_3 (ns)	$<\tau_\alpha>$ (ns)
ISO	475	720	0.53	0.27	0.2	1.68	1.09	0.06	1.20
		780	0.19	0.67	0.14	1.41	0.89	0.08	0.88
4X		720	0.31	0.56	0.13	1.87	1.22	0.12	1.29
		780	0.06	0.81	0.13	1.18	0.81	0.06	0.74

PVA	Excitation (nm)	Observation (nm)	α_1 (%)	α_2 (%)	α_3 (%)	τ_1 (ns)	τ_2 (ns)	τ_3 (ns)	$<\tau_\alpha>$ (ns)
ISO	510	720	0.44	0.18	0.38	1.61	0.89	0.03	0.88
		780	0.30	0.23	0.47	1.08	0.72	0.02	0.50
4X		720	0.32	0.44	0.24	1.73	1.03	0.08	1.03
		780	0.47	0.23	0.3	0.98	0.65	0.03	0.62

PVA	Excitation (nm)	Observation (nm)	α_1 (%)	α_2 (%)	α_3 (%)	τ_1 (ns)	τ_2 (ns)	τ_3 (ns)	$<\tau_\alpha>$ (ns)
ISO	730	780	0.05	0.03	0.92	1.07	0.66	0.003	0.08
4X		780	0.18	0.04	0.78	0.97	0.58	0.008	0.20

α_n – Percent intensity amplitude

From the results shown in Table 2, we did not observe a significant change in the fluorescence lifetime time when we used different excitations, which was expected since PD was in the same environment, PVA.

Next, we selected 475 nm excitation that preferentially excites the twisted form and measured fluorescence lifetimes in EtOH (low viscosity) and glycerol (high viscosity).

Table 3 presents the measured fluorescence lifetimes and their corresponding amplitudes. For comparison, we also included measured values for solid PVA film (no conformational change allowed).

Table 3: Fluorescence lifetime of PD in Ethanol, Glycerol, and PVA.

Excitation: 475 nm	Media	Observation / nm	A_1	A_2	A_3	τ_1/ ns	τ_2/ ns	τ_3/ ns
	Ethanol	720	$86 * 10^3$	$5.1* 10^3$	$1.5* 10^3$	0.08	0.38	1.38
		780	$-29* 10^3$	$47* 10^3$	$3.7* 10^3$	**0.02**	0.37	0.59
	Glycerol	720	$23* 10^3$	$24* 10^3$	$9.2* 10^3$	0.23	0.59	2.10
		780	$17* 10^3$	$31* 10^3$	$.79* 10^3$	0.23	0.50	1.61
	PVA	720	$3.2* 10^3$	$3.1* 10^3$	$9.2* 10^3$	0.06	0.98	1.64
		780	$2.1* 10^3$	$9.6* 10^3$	$3.1* 10^3$	0.08	0.88	1.42

τ_n – lifetime component

A_n – Intensity amplitude (It is not possible to obtain the percent intensity amplitude nor the average intensity lifetime due to the negative component).

For low viscosity (ethanol) we observed a large negative component with a 20 ps fluorescence lifetime. This negative component represents the molecules that are populating the ensemble of planar conformation excited molecules after the pulse's excitation. This reflects a positive pre-exponential decay (or population increase) in the exponential decay function. Importantly, in Table 2, we did not experience the negative lifetime component similar to

Table 3. This indicates there was not energy transfer between the two conformers that was due to the conformational change in its excited state. This observation was expected when PD was embedded in a solid matrix, and a change in its conformation is forbidden. Furthermore, the twisted conformation exhibited a longer average fluorescence lifetime as compared to the planar conformer.

5.8 Conclusions

The system of Porphyrin Dimer consists of physical properties that well-represent a typical molecular rotor system. In this work, we have conducted a detailed spectroscopic study model of the PD system, which can also be applied to other molecular rotor systems. Specifically, we measured linear dichroism of PD molecules in oriented PVA films and determined the electronic transition moment orientations for major optical transitions. These studies of PD have been the first attempt to orient a dimeric molecular system in a PVA matrix. We further discovered that by using a heat-assisted mechanical force to stretch the PVA films that were doped with PD to their stretching limit (4 times the original length), we were able to force the PD molecules to a single (planar) conformation. The ability to orient the PD molecules and shift them towards a single conformation allows us to exhibit the unknown-transitions associated with their planar or twisted conformations.

The results from linear dichroism studies indicated a domination at the long-wavelength edge of the Soret absorption band (470 nm -480 nm) by a strong transition belonging to the twisted conformation molecules. At 500 nm, PD exhibits a transition oriented along the long molecular axis. In the Q-bands, the long wavelength transition at about 780 nm oriented along a long molecular axis, while the shorter wavelength transition at about 720 nm oriented orthogonal to the long molecular axis. Those results further confirmed the utilization of the 475 nm excitation to preferably populate (excite) the twisted form and evaluate the viscosity of a given solvent by using the ratio of emission between twisted and planar (710 nm/780 nm) forms. Also, the stretching degree of the PD/PVA films (from non-stretched to 4 times the original length) was strongly correlated with the percentage of the planar conformation in the system. The correlation suggests

a future application of utilizing heat-assisted mechanical force and molecular rotor system in the PVA matrix in developing a force sensor. Specifically, the amount of applied force in stretching the PVA film doped with the molecular rotor can be possibly associated with the percentage of the planar conformer of the system.

The steady-state emission studies of PD in different viscosity solvents have shown that emission predominantly originates from the lower energy planar form at 780 nm. However, when we increased the solvent viscosity, we detected an increased contribution from the twisted form's emission at 720 nm. In addition to the emission studied of PD in solvents, the emission of PD in non-stretched and heat-assisted stretching PVA films helps us assign separately the emission spectra associated with the twisted and planar conformations. The twisted form of PD emits at 710 nm, and the planar form emits at 780 nm. The result plays an important step in studying PD as a photosensitizer due to their different interactions with the molecular oxygen to generate the ROS species in PDT.

Lastly, time-resolved studies of PD in different viscosity solvents demonstrated that the planar form is populated through the molecular transition from a twisted form to a planar form. The transition occurred in the excited state as a rapid process. For the first time, we observed such a transition live in the excited state, as expressed by a negative lifetime intensity component with a 20 ps fluorescence lifetime. Furthermore, we were able to distinguish the difference in fluorescence lifetime of the two conformers. The twisted form exhibits a longer fluorescence lifetime as compared to the planar form. Those results are significant for using this molecular system as the molecular rotor (micro-viscometer) since the transition from one form to another provides critical information about the viscosity of the environment.

Bibliography

1. Jameson LP, Kimball JD, Gryczynski Z, Balaz M, Dzyuba SV. Effect of ionic liquids on the conformation of a porphyrin-based viscometer. *RSC Advances*. 2013;3(40):18300-18304.

2. Jameson LP, Balaz M, Dzyuba SV, Kamiya N. Conformational preference of a porphyrin rotor in confined environments. *RSC Advances*. 2014;4(2):705-708.

3. Collins HA, Khurana M, Moriyama EH, et al. Blood-vessel closure using photosensitizers engineered for two-photon excitation. *Nature Photonics*. 2008;2(7):420.

4. Balaz M, Collins HA, Dahlstedt E, Anderson HL. Synthesis of hydrophilic conjugated porphyrin dimers for one-photon and two-photon photodynamic therapy at NIR wavelengths. *Organic & biomolecular chemistry*. 2009;7(5):874-888.

5. Kuimova MK, Botchway SW, Parker AW, et al. Imaging intracellular viscosity of a single cell during photoinduced cell death. *Nature Chemistry*. 2009;1(1):69-73.

6. Dahlstedt E, Collins HA, Balaz M, et al. One-and two-photon activated phototoxicity of conjugated porphyrin dimers with high two-photon absorption cross sections. *Organic & biomolecular chemistry*. 2009;7(5):897-904.

7. Bonnett R, Martinez G. Photobleaching studies on azabenzoporphyrins and related systems: A comparison of the photobleaching of the zinc (II) complexes of the tetrabenzoporphyrin, 5-azadibenzo [b, g] porphyrin and phthalocyanine systems. *Journal of Porphyrins and Phthalocyanines*. 2000;4(05):544-550.

8. Dolmans DE, Fukumura D, Jain RK. Photodynamic therapy for cancer. *Nature reviews cancer*. 2003;3(5):380.

9. Niedre M, Patterson MS, Wilson BC. Direct near-infrared luminescence detection of singlet oxygen generated by photodynamic therapy in cells in vitro and tissues in vivo. *Photochem Photobiol*. 2002;75(4):382-391.

10. Vrouenraets MB, Visser GW, Snow GB. Basic principles, applications in oncology and improved selectivity of photodynamic therapy. *Anticancer Res*. 2003;23(1B):505-522.

11. Allison RR, Downie GH, Cuenca R, Hu X, Childs CJ, Sibata CH. Photosensitizers in clinical PDT. *Photodiagnosis and photodynamic therapy*. 2004;1(1):27-42.

12. Bowser MT, Sternberg ED, Chen DD. Quantitative description of migration behavior of porphyrins based on the dynamic complexation model in a nonaqueous capillary electrophoresis system. *Electrophoresis*. 1997;18(1):82-91.

13. Oleinick, Nancy L., Rachel L. Morris, Irina Belichenko. The role of apoptosis in response to photodynamic therapy: What, where, why, and how. *Photochemical & Photobiological Sciences*. 2002;1:1-21.

14. Kolarova H, Nevrelova P, Tomankova K, Kolar P, Bajgar R, Mosinger J. Production of reactive oxygen species after photodynamic therapy by porphyrin sensitizers. *Gen Physiol Biophys*. 2008;27(2):101.

15. Norden B. *Circular dichroism and linear dichroism.* Vol 1. Oxford University Press, USA; 1997.

16. Norden B, Kubista M, Kurucsev T. Linear dichroism spectroscopy of nucleic acids. *Q Rev Biophys*. 1992;25(1):51-170.

17. Thulstrup EW, Downing JW, Michl J. Excited singlet states of pyrene. polarization directions and magnetic circular dichroism of azapyrenes. *Chem Phys*. 1977;23:307-319.

18. THULSTRUP EW, MICHL J. Orientation and linear dichroism of symmetrical aromatic molecules imbedded in stretched polyethylene. *ChemInform*. 1983;14(3).

19. Thulstrup EW, Michl J. Polarized absorption spectroscopy of molecules aligned in stretched polymers bl. *Spectrochim Acta, Pt A: Mol Spectrosc*. 1988;44(8):767-782.

20. Lakowicz JR. Principles of frequency-domain fluorescence spectroscopy and applications to cell membranes. In: *Fluorescence studies on biological membranes.* Springer; 1988:89-126.

21. Zielinski TJ, Harvey E, Sweeney R, Hanson DM. No title. *Quantum states of atoms and molecules*. 2005.

22. Tanizaki Y. Dichroism of dyes in the stretched PVA sheet. II. the relation between the optical density ratio and the stretch ratio, and an attempt to analyse relative directions of absorption bands. *Bull Chem Soc Jpn*. 1959;32(1):75-80.

23. Tanizaki Y. The correction of the relation of the optical density ratio to the stretch ratio on the dichroic spectra. *Bull Chem Soc Jpn*. 1965;38(10):1798-1799.

24. Kawski A, Gryczyński Z. On the determination of transition-moment directions from emission anisotropy measurements. *Zeitschrift für Naturforschung A*. 1986;41(10):1195-1199.

25. Becker W. *The bh TCSPC handbook.* Becker & Hickl; 2014.

26. Grinvald A, Steinberg IZ. On the analysis of fluorescence decay kinetics by the method of least-squares. *Anal Biochem*. 1974;59(2):583-598.

27. Badea MG, Brand L. [17] time-resolved fluorescence measurements. *Meth Enzymol*. 1979;61:378-425.

28. Ware WR, Doemeny LJ, Nemzek TL. Deconvolution of fluorescence and phosphorescence decay curves. least-squares method. *J Phys Chem*. 1973;77(17):2038-2048.

29. O'Connor DV, Ware WR, Andre JC. Deconvolution of fluorescence decay curves. A critical comparison of techniques. *J Phys Chem*. 1979;83(10):1333-1343.

30. Joseph RL, Lakowicz R. Principles of fluorescence spectroscopy. . 1999.

31. Dougherty TJ, Gomer CJ, Henderson BW, et al. Photodynamic therapy. *JNCI: Journal of the National Cancer Institute*. 1998;90(12):889-905.

32. Pandey RK, Zheng G. Porphyrins as photosensitizers in photodynamic therapy. *The porphyrin handbook*. 2000;6:157-230.

33. Gouterman M. Optical spectra and electronic structure of porphyrins and related rings. *The porphyrins*. 1978;3.

34. Senge MO, Ryan AA, Letchford KA, MacGowan SA, Mielke T. Chlorophylls, symmetry, chirality, and photosynthesis. *Symmetry*. 2014;6(3):781-843.

35. Weaver JJ. Weaver J john thesis. *Thesis by Jeremy John Weaver*. 2005.

36. Collins HA, Khurana M, Moriyama EH, et al. Blood-vessel closure using photosensitizers engineered for two-photon excitation. *Nature Photonics*. 2008;2(7):420.

37. Weissleder R. Ralph weissleder 2001. *A clearer vision for in vivo imaging*. 2001.

38. Ochsner M. Light scattering of human skin: A comparison between zinc (II)—phthalocyanine and photofrin II®. *Journal of Photochemistry and Photobiology B: Biology*. 1996;32(1-2):3-9.

39. Luchowski R, Sarkar P, Bharill S, et al. Fluorescence polarization standard for near infrared spectroscopy and microscopy. *Appl Opt*. 2008;47(33):6257-6265.

40. Mukerjee A, S�rensen TJ, Ranjan AP, Raut S. A mukerjee, T J s�rensen, A P ranjan and S raut and gryczynski Z. *J Phys Chem B*. 2010;2010:114.

41. Doan H, Raut SL, Yale D, Balaz M, Dzyuba SV, Gryczynski Z. Mechanothermally induced conformational switch of a porphyrin dimer in a polymer film. *Chemical Communications*. 2016;52(61):9510-9513.

42. Vyšniauskas A, Balaz M, Anderson HL, Kuimova MK. Dual mode quantitative imaging of microscopic viscosity using a conjugated porphyrin dimer. *Physical Chemistry Chemical Physics*. 2015;17(11):7548-7554.

43. Jameson LP, Kimball JD, Gryczynski Z, Balaz M, Dzyuba SV. Effect of ionic liquids on the conformation of a porphyrin-based viscometer. *RSC Advances*. 2013;3(40):18300-18304.

Curriculum Vitae

Hung The Doan
Fort Worth, Texas. USA
hung.doan@tcu.edu +1(682)521-0280/ +1(469)702-0990

Personal Background

Hung The Doan
Hue, Vietnam
Son of Hieu Doan, Ph.D. and Phuong Huyen

Education

- Doctor of Philosophy (Ph.D.) in Biophysics — 2018
  Department of Physics & Astronomy
  Texas Christian University
  Fort Worth, Texas, USA

- MBA Business Option for Ph.D. Candidate — 2018
  Neeley School of Business
  Texas Christian University
  Fort Worth, Texas, USA

- Bachelor of Science in Physics — 2013
  Minor: Mathematics & Chemistry
  John V. Roach Honors College
  Texas Christian University
  Fort Worth, Texas, USA

- Diploma - Quoc Hoc High School — 2006
  Hue, Vietnam

Experiences

- Research Assistantship, Texas Christian University — 2013-2017
  Development of Fluorescence Technology
  Advisor: Dr. Zygmunt Gryczynski
  Fort Worth, TX, USA

- Teaching Assistantship, Texas Christian University — 2013-2017
  General Physics 1 & 2 Lab (Physics & Non-Physics Major)
  Fort Worth, TX, USA

- Student Research Volunteer, UNT Health Science Center — 2011-2017
  Center for Fluorescence Technologies and Nanomedicine
  Advisor: Dr. Zygmunt Gryczynski
  Fort Worth, TX, USA

- Undergraduate Research, Texas Christian University — 2011-2013
  Development of Fluorescence Technology
  Advisor: Dr. Zygmunt Gryczynski
  Fort Worth, TX, USA

Abstract

A STUDY OF THE ELECTRONIC TRANSITIONS OF A PORPHYRIN DIMER

By Hung The Doan, 2018

Department of Physics and Astronomy

Texas Christian University

Dissertation Advisor:

Dr. Zygmunt K. Gryczynski, "Tex" Moncrief Jr. Chair Professor of Physics

“Porphyrin Dimer” (PD) is a recently developed porphyrin derivative that consists of two conjugated porphyrin units. PD presents favorable photophysical properties to be utilized as a photosensitizer in photodynamic therapy (PDT), such as a high extinction coefficient, good photostability, and shows high intracellular accumulation. Furthermore, these two porphyrin moieties have the unique ability to rotate around its diyne moiety, thus forming a so-called “molecular rotor.” This physical process (rotation) from planar to non-planar conformation (and vice-versa) is associated with a significant change in its molecular orbitals and presents an easily detectable change in its absorption and fluorescence properties. Importantly, the rings’ rotation can be robustly hindered by their surroundings, and especially the solvent’s microviscosity. Therefore, the PD molecular rotor is highly capable of reporting on its local environment’s viscosity.

To fully utilize PD as a cellular viscometer (rotor) and potentially as a photosensitizer in PDT, this study focuses on exploring the unknown characteristics and photophysical properties of both PD’s major conformations. The main goal is to establish a new and robust method to determine the unknown orientation and relative strengths of the transition moments for the planar and twisted conformers of PD. This required first to immobilize and orient PD molecules using solid matrices

and then force PD's molecules toward one dominant conformation (planar or twisted). The next step is to utilize methods to study the orientation of transition moments for absorption (linear dichroism – "LD") and emission (fluorescence anisotropy) of the dominant conformer and identify the electronic transitions that are most suitable for the PD to be used as a molecular rotor. In addition, the study also aims to understand the rationals behind the widely used excitation in the 470 nm to 480 nm range in utilizing PD as a molecular rotor. These properties are likely to play a fundamental role in optimizing molecular systems to be used as molecular rotors or as a photosynthesizer for PDT, and the development of the next generation of rotors and photosensitizers.